Accepted Manuscript

Geothermal Studies of the Outokumpu Deep Drill Hole, Finland: Vertical variation in heat flow and palaeoclimatic implications

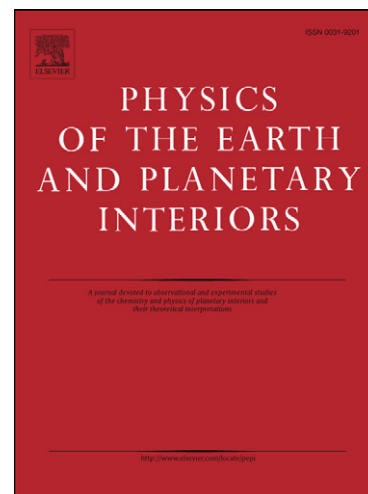Ilmo T. Kukkonen, Volker Rath, Liisa Kivekäs, Jan Šafanda, Vladimir Čermak

Please cite this article as: Kukkonen, I.T., Rath, V., Kivekäs, L., Šafanda, J., Čermak, V., Geothermal Studies of the Outokumpu Deep Drill Hole, Finland: Vertical variation in heat flow and palaeoclimatic implications, *Physics of the Earth and Planetary Interiors* (2011), doi: 10.1016/j.pepi.2011.06.002

1

1
2
3
4
5
6 **Geothermal Studies of the Outokumpu Deep Drill Hole, Finland:**

7 **Vertical variation in heat flow and palaeoclimatic implications**

8

9 **Ilmo T. Kukkonen[1*], Volker Rath[2], Liisa Kivekäs[1],**

10 **Jan Šafanda[3] & Vladimir Čermak[3]**

11

12 [1]Geological Survey of Finland, P.O.B. 96, FI-02151, Espoo, Finland

13 (ilmo.kukkonen @gtk.fi)

14 *corresponding author

15 Tel +358-205502270

16 Fax +358-2015012

17

18 [2] Dpto. Astrofísica y CC. de la Atmósfera, Facultad CC. Físicas, Universidad

19 Complutense de Madrid, Madrid, Spain

20

21 [3]Institute of Geophysics, Czech Academy of Science, Bocni II, Prague,

22 Czech Republic

23

24

25

26 Manuscript

27 August 2, 2010

28 Revised June 7, 2011

29

30 **Abstract**

31

32 Detailed geothermal studies of deep drill holes provide insights to heat transfer

33 processes in the crust, and allow separation of different factors involved, such as

34 palaeoclimatic and structural conductive effects as well as advective fluid flow

35 effects. We present high resolution geothermal results of the 2,516 m deep

36 Outokumpu Deep Drill Hole in eastern Finland drilled in 2004-2005 into a

37 Palaeoproterozoic formation with metasedimentary rocks, ophiolite-derived altered

38 ultramafic rocks and pegmatitic granite. The down-hole temperatures have been

39 logged five times after end of drilling and extend to day 948 after drilling. The hole is

40 completely cored (79% core coverage) and thermal conductivity measurements were

41 done at 1 m intervals. The geothermal results on temperature gradient, thermal

42 conductivity and heat flow density yield an exceptionally detailed data set and

43 indicate a significant vertical variation in gradient and heat flow density. Heat flow

44 density increases from about 28-32 mW m^{-2} in the uppermost 1000 m to 40-45 mW

45 m^{-2} at depths exceeding 2000 m. The estimated undisturbed surface heat flow value is

46 42 mWm^{-2}. We present results on forward and inverse transient conductive models

47 which suggest that the vertical variation in heat flow can mostly be attributed to a

48 palaeoclimatic effect due to ground surface temperature (GST) variations during the

49 last 100,000 years. The modelling suggests that the average GST was about -3…-4°C

50 during the Weichselian glaciation. Holocene GST values are within ±2 degree from

51 the present average GST in Outokumpu (5°C). The topographic hydraulic heads and

52 hydraulic conductivity of crystalline rocks are low which suggests that advective heat

53 transfer in the formation is not significant. The slow replacement of fresh flushing

54 water by saline formation fluids is observed in the hole, but it does not generate

55 significant thermal disturbances in the logs. On the other hand, free sluggish thermal

56 convection is present in the large diameter (22 cm) borehole, and temperature

57 variations in the range of few mK to 0.01 K occur over times of minutes to tens of

58 minutes. Theory suggests that convection cells are about as tall as the drill hole

59 diameter, and thus the free convection is expected to generate only local thermal

60 'noise' not affecting the general geothermal results.

61

64   **1. Introduction**

65

66   A deep research borehole was drilled in 2004-2005 in eastern Finland by the

67   Outokumpu Deep Drilling Project of the Geological Survey of Finland (GTK). The

68   2,516 m deep hole was drilled into a Palaeoproterozoic metasedimentary, igneous and

69   ophiolite-related sequence of rocks in a classical ore province with massive Cu-Co-Zn

70   sulphide deposits (Fig. 1). The Outokumpu DDP (Deep Drilling Project) is carried out

71   in an international framework, partly supported by International Continental Scientific

72   Drilling Program (ICDP). The aims and results of the drilling project as a whole and

73   the different subprojects are discussed in details in (Kukkonen, 2009; 2011). GTK

74   used the company NEDRA (Jaroslavl, Russia) as the drilling contractor.

75

76   Geothermal studies are an essential component of the Outokumpu DDP. In

77   geothermics, the near-surface disturbances should be avoided as far as possible, and

78   therefore the depth reached in drilling and logging is always a value of itself. Only in

79   a deep hole it is possible to directly recognize systematic vertical variations in

80   temperature gradient and heat flow density due to long-term paleoclimatic

81   disturbances, groundwater flow and structural effects. In the super-deep drilling

82   project in the Kola Peninsula, Russia (Kremenetsky and Ovchinnikov, 1986) and the

83   KTB holes in southern Germany (Clauser et al., 1997), an important argument in

84   deciding the deep drilling sites was the low geothermal gradient suggested by shallow

85   holes. However, the final hole temperatures and deep gradients measured in both

86   drilling projects clearly exceeded the predictions. If such results would represent the

87   common crustal conditions, they would have dramatic implications for correcting and

88   using shallow (< 1 km) heat flow data for calculating crustal and lithospheric

89   temperatures. Ever since the geothermal results of the Kola hole became known in the

90   late 1980's (Kremenetsky and Ovchinnikov, 1986), there has been a discussion on the

91   existence and causes of vertical heat flow variation in the continental upper crust as

92   well as need for and reporting of new experimental data (Kukkonen and Clauser,

93   1994; Clauser et al., 1997; Kukkonen et al., 1997,1998; Popov et al., 1998a,b,

94   1999a,b; Kukkonen and Jõeleht, 2003; Glaznev et al., 2004; Šafanda et al., 2004;

95   Majorowicz and Šafanda, 2007; Mottaghy et al., 2005; Majorowicz and Wybraniec,

96   2010).

97

98   From the geothermal viewpoint, the Outokumpu Deep Drill Hole provides one of the

99   deepest undisturbed temperature and heat flow density profiles in the uppermost 2.5

100   km. In the Fennoscandian Shield, there are not many boreholes reaching such depths

101   with detailed geothermal observations. Holes down to about 1 km level are relatively

102   common, but in Fennoscandia holes deeper than the Outokumpu hole are only the

103   Kola super-deep hole in Russia (12.3 km; e.g. Kremenetsky and Ovchinnikov, 1986),

104   the two Siljan holes (6 and 7 km; Balling et al., 1990) in central Sweden, and the

105   recently finished Onetshkaya hole in Russian Karelia (3.5 km; Y.M. Erinchek, written

106   comm., 2008). Detailed geothermal results have so far been published only on the

107   Kola Super-Deep (Popov et al., 1999a,b). The Kola super-deep hole indicated that

108   there is a significant increase in heat flow density in the uppermost 1-3 km of crust

109   (Kremenetsky and Ovchnnikov, 1986). Similar results have been obtained in the KTB

110   deep holes in Germany (Clauser et al., 1997), in the Udryn and Torun holes in Poland

111   (Šafanda et al., 2004; Majorowicz and Šafanda, 2007), and in the central Kola

112   Peninsula (Glaznev et al., 2004). As the common heat flow maps (e.g. Hurtig et al.,

113   1992) are based to a great deal on holes shallower than 1 km, the vertical variation in

114   heat flow is a crucial issue for applications of geothermal data in crustal studies.

115

116   Our motivations for the geothermal investigations in the Outokumpu hole are (1) to

117   investigate whether there is a vertical variation in heat flow density, and if so, to

118   determine the magnitude of the variation as well as to find out what are the factors

119   causing such variation; (2) to study the effects of past climate on the subsurface

120   thermal regime and to invert ground surface temperature histories covering the last

121   100,000 years; (3) to study to what degree the thermal conditions may be disturbed by

122   advective heat transfer (fluid flow); and (4) whether there is free thermal convection

123   of fluid in the large diameter drill hole affecting the high resolution temperature logs.

124

125   We present geothermal results based on nine temperature logs measured during and

126   after drilling, and on more than 1,900 thermal conductivity measurements of the drill

127   core as well as theoretical modelling of the data.

128

129

130

131

132 **2. The Outokumpu drilling site and structures intersected**

133

134 The Outokumpu Deep Drilling site is located 2.5 km SE of the old Outokumpu

135 mining town in eastern Finland at 62° 43' 02.63" N, 29° 03' 55.01"E (Fig. 1). The

136 area is well-known for its massive and semi-massive Cu-Co-Zn sulphide deposits

137 mined from about 1910 to 1984. The Outokumpu belt is one of the oldest (1.95 Ga)

138 known ophiolite systems (Säntti et al., 2006; Peltonen et al., 2008). One of the aims of

139 the deep hole was to reveal the geological nature of the strong seismic reflectors

140 dominating the upper crust in the Outokumpu area (Kukkonen et al., 2006; 2011). The

141 deep hole was targeted to intersect one of the uppermost strong reflectors which

142 proved to be packages of ophiolite-derived rock types (serpentinite, diopside-tremolite

143 skarn, quartz rock, i.e. the typical host rocks of the Outokumpu type sulphide

144 deposits) and black schist in a metasedimentary host rock (metaturbiditic mica schist).

145 At deeper levels of the hole pegmatitic granite dominates the drilled section (Fig. 2).

146

147 The hole was drilled with continuous coring, and the final core coverage was 79 %,

148 with the main core losses occurring at zones of heavy fracturing and shearing. The

149 most common rock types in the deep hole are mica schist and pegmatitic granite,

150 which form together more than 90 % of the drilled section. Rock types of the

151 ophiolite-related Outokumpu assemblage form about 8 % of the section (Fig. 2). The

152 seismic data suggested that the structures are mostly horizontal or dipping at very low

153 angles at the drilling site which was confirmed by the drill core. 3D-visualization of

154 the high-resolution seismic data further suggests that the structures are quite 2-

155 dimensional in the direction of the main ore belt (Fig. 3).

156

157 The hole is cased to the depth of 39 m (casing inner diameter 324 mm), below which

158 the hole is uncased and has a nominal diameter of 220 mm. The casing was cemented

159 to the sediments and bedrock. Local tap water was used as drilling mud which was

160 occasionally thickened with peat and bentonite to increase its viscosity at zones of

161 unstable rocks to generate a mud-cake on the walls (especially at 520-850 m).

162 Cementing was used at 75-274 m to stabilize the hole walls.

163

164 The drilling phase took 302 days (April 6, 2004 – January 31, 2005). The temperature

165 of the drilling mud, which was circulated back to the hole after removal of cuttings,

166 was monitored daily. Also the total consumption of water on the drilling site was

167 recorded (Ahonen et al., 2011).

168

169 **3. Down-hole logging of in-situ temperature and lab measurements of thermal**

170 **properties**

171

172 Temperature logs were obtained in several stages during and after drilling (Table 1).

173 During drilling breaks at every 500 m of accomplished depth the hole was logged by

174 the NEDRA logging team with about 20 different geophysical down-hole tools, one

175 of them temperature. This way four continuous temperature logs with reading interval

176 of 0.2 m were obtained after shut-in times of 1-2 days. The applied temperature tool

177 had a resolution of 0.01 K and it was calibrated by the contractors to be better than 0.1

178 K. At end of drilling the drill hole was flushed clean with tap water, and the

179 temperature was logged after 7 days of shut-in time by the NEDRA team. During

180 shut-in time during drilling breaks, the down-hole logs and fluid sampling were the

181 only activities in the hole.

182

183 Post-drilling temperature logs were obtained first in August 31, 2005 (211 days shut-

184 in time) by the geothermal team of the Geophysical Institute of the Czech Academy of

185 Sciences. The used temperature probe was a memory logger probe (Antares Gmbh)

186 with a resolution of 0.001 K and an absolute accuracy of better than 0.05 K. The log

187 was obtained by point-by-point readings at 5 m intervals. This log extended to only

188 1450 m depth. Thereafter several temperature logs were measured by the logging

189 team of the ICDP Operational Support Group in 2006 and 2008. These were done on

190 April 6, 2006 (433 days shut-in time), September 20, 2006 (597 days) and September

191 5, 2008 (948 days). The used mud-parameter tool measures simultaneously

192 temperature and fluid electrical resistivity. The continuous logs measured with

193 reading interval of 0.1 m have a resolution of 0.01 K and an absolute accuracy of

194 better than 0.1 K. The temperature logging history is summarized in Table 1.

195

196 Other activities in the hole during the post-drilling time included sampling of the drill

197 hole water with a tube method in 2007 and 2008 (Ahonen et al., 2011), and hydraulic

198 difference-flow measurements (in the uppermost 1290 m in August 2007; Sokolnickni

199   and Heikkinen, 2008). These operations lasted less than 4 weeks altogether, and are

200   considered to have had no detectable effects on the temperature logs.

201

202   In addition to the down-hole data, the water table level is monitored automatically by

203   GTK in the deep hole as well as the ground temperatures and water levels in a shallow

204   (17 m deep) hole in the Quaternary overburden (Hänninen et al., 2009). This data

205   provided useful additional information on the hydrogeological condition of the hole

206   and shows that the deep hole water is not in a hydraulic connection with the shallow

207   sediments.

208

209   Thermal conductivity was measured on drill core samples at about 1 m intervals with

210   the total number of samples being 1922. The laboratory measurement required drilling

211   of a new specimen from the original 6-10 cm diameter cores, and finally 7 mm thick

212   disks with 42 mm diameter were cut and polished. The disks were immersed in tap

213   water for minimum duration of two days to saturate open pores and micro-fractures,

214   and thermal conductivity was subsequently measured at room temperature with a

215   divided bar instrument constructed at GTK (Kukkonen and Lindberg, 1998). The

216   instrument applies quartz references (conductivity in direction of crystallographic a-

217   axis) in the bar and the measurements are controlled by comparison with low-

218   conductivity Duran glass and high conductivity quartz (conductivity in direction of

219   crystallographic c-axis). The inaccuracies of the measurements are smaller than 5 %

220   (Kukkonen and Lindberg, 1998).

221

222   The specific heat capacity was measured with a calorimetric method using a subset of

223   conductivity disks at about 100 m depth intervals. The samples were pre-heated in

224   boiling water, and then immersed into room temperature water in a calorimeter. The

225   measurements have inaccuracies below 5 %, and the results were corrected to ambient

226   temperature (Kukkonen and Lindberg, 1998). Bulk density for diffusivity

227   determination was determined by the Archimedean principle by weighing the samples

228   in water and air. The obtained accuracy is better than about 0.2 % for samples with

229   masses of ca. 25 g (typical for conductivity disks used).

230

231

232 **4. Results: Temperature gradient, thermal conductivity, heat production and**
233 **heat flow density**

234

235 The logs taken during drilling breaks show a very strong deviation from equilibrium
236 temperatures. The ski-shaped logs differ by about 10-15 degrees at maximum from
237 undisturbed values, excluding the lowermost readings of each log, which were least
238 disturbed by mud circulation (Fig. 4). The post-drilling logs show a rapid
239 equilibration towards undisturbed formation temperatures, and the latest temperature
240 log measured in September 2008 is already very close to equilibrium. In the
241 uppermost parts of the hole where the disturbance is biggest, numerical modeling
242 suggests that temperatures are already within ~ 0.1 °C of the equilibrium
243 temperatures.

244

245 At end of drilling, the borehole was flushed clean and filled with fresh tap water.
246 Subsequently, the electrical conductivity (representing fluid salinity) of the drilling
247 fluid has gradually increased which suggests slow inflow of formation fluid from a
248 restricted number of fractures (Fig. 5). However, the rate of fluid flow is very small,
249 and does not seem to play a role in heat transfer that could be seen in the temperature
250 logs.

251

252 Temperature gradient shows a distinct vertical increase from about 13-14 mK m^{-1} at
253 50 m – 1.3 km (in the upper mica schist unit), lower but more variable values of 10-13
254 mKm^{-1} at 1.3-1.5 km (in the ophiolite-derived rocks), and about 16 mK m^{-1} in the
255 lower mica schist unit and pegmatitic granite at 1.5 – 2.2 km. In the lowermost part of
256 the hole at 2.2 – 2.5 km temperature gradient shows lower but variable values in the
257 range of 13-16 mK m^{-1} (Fig. 6).

258

259 Thermal conductivity shows small-scale variation with typical standard deviation of
260 about 0.5 Wm^{-1}K^{-1} which we attribute to normal geological heterogeneity between
261 small samples. However, when a moving average (20-m window) is calculated,
262 thermal conductivity is very stable in the mica schist and pegmatitic granite (Fig. 6).
263 In the mica schist average thermal conductivity is 2.5 Wm^{-1}K^{-1}. The foliated rock is
264 thermally anisotropic, but the (sub)horizontal orientation of foliation in the drilled
265 section results in relatively low conductivity values as the conductivity is measured in

266 a direction perpendicular to schistosity and foliation. In the pegmatitic granite,
267 average conductivity is 3 $Wm^{-1}K^{-1}$. Higher but variable values of conductivity are
268 associated to the Outokumpu assemblage of rock types with peaks up to 10 $Wm^{-1}K^{-1}$
269 but the average is 3.35 $Wm^{-1}K^{-1}$. The generally elevated values are due to tremolite
270 and diopside bearing skarn rocks and the peak values to the presence of talc in
271 serpentinites as well as graphite in black schists enveloping the ophiolitic rocks.

272

273 Radiogenic heat production was determined according to Rybach (1973) from the
274 neutron density log and the U, Th and K channels of the natural gamma ray
275 spectrometric logs measured by NEDRA. The results show a practically constant heat
276 production value in the mica schist (mean 1.7 $\mu W\ m^{-3}$), high values in the pegmatitic
277 granite (mean 5.4 $\mu W\ m^{-3}$), and sharp variations in the altered ultrabasic rocks of the
278 ophiolite-derived rock types. Namely, the serpentines have practically negligible heat
279 production levels whereas the skarn rocks show values up to 6-7 $\mu W\ m^{-3}$. The average
280 heat production of the ophiolitic rocks is 1.55 $\mu W\ m^{-3}$.

281

282 When combined with temperature measurements, a very detailed heat flow density
283 profile could be constructed (Fig. 6). Heat flow density was determined in two ways,
284 first, as the product of the moving averages (20 m windows) of thermal conductivity
285 and temperature gradient, and second, as the product of average conductivity and
286 gradient calculated in 100 m depth sections (Fig. 6 and Table 1). A systematic vertical
287 increase in heat low density is observed. Heat flow increases from about 30 mW m^{-2}
288 in the uppermost 1 km to about 40-45 mW m^{-2} at depths beneath 1.5 km.

289

290 **5. Conductive vs. advective heat transfer**

291

292 *Flow systems between borehole and fractures.* Generally, the Outokumpu temperature
293 logs seem to represent a thermal regime characterized mainly by conductive heat
294 transfer with practically no apparent indications of fluid flow disturbances in the hole.
295 Nevertheless, there is slow flow of fluid into and out from the hole. This is indicated
296 by the fluid electrical conductivity logs (Fig. 5). The fresh fluid used in final flushing
297 of the hole at end of drilling had an electrical conductivity of about 2.5 mS/cm. The
298 subsequent repeated logs of fluid electrical conductivity indicate gradual changes in
299 borehole fluid salinity and suggest slow inflow of formation fluid from a restricted

300 number of fractures (Fig. 5). The driving force of this flow is very likely the density

301 difference between the fresh flushing water and the saline formation fluids. Density is

302 about 1.00 g/cm^3 in the fresh and 1.04 g/cm^3 in the most saline fluids, respectively.

303

304 The fluid electrical conductivity seems to have reached a semi-stable condition at the

305 uppermost parts of the hole, but in the lower parts the salinity keeps increasing even at

306 the time of the latest log (Sept 2008, 948 days after drilling). A qualitative

307 interpretation of the flow from and into fractures is presented in Fig. 5. At the depths

308 of the most important in-flow points, the temporal fluid salinity changes show the

309 development of mixing. At the time of the last log in 2008 the salinity seems to have

310 already stabilized at 967 m, whereas at 1,715 m the salinity is still slowly increasing,

311 but at 2,300 and 2,435 m the salinity keeps increasing more or less linearly with time.

312 This indicates the slow replacement of fresh drill hole water by the saline formation

313 fluids, and also implies that the formation fluids become more saline with depth. The

314 order of magnitude of flow rate into the hole can be estimated by calculating the

315 dilution of the fluids using the depth ranges of the indicated flow systems along the

316 hole (~100-1000 m, Fig. 5), the corresponding fluid volumes and time past after the

317 end of drilling. These calculations suggest that the flow rates of formation fluid into

318 the hole are in the range of 0.4 – 0.04 ml/s.

319

320 The thermal effects of flow between the formation and borehole have been studied

321 theoretically by Ramey (1962), Drury and Lewis (1983) and Drury (1984). At the

322 depth of flow into the hole the temperature anomaly is very gradual, particularly if the

323 fluid has no temperature contrast with the prevailing formation temperature. When

324 flowing along the hole, the fluid heats or cools depending on the geothermal gradient,

325 flow rate and direction, and the thermal properties of fluid and rock. As a result a

326 deviation from undisturbed temperatures is developed. However, at the depth of flow

327 out from the hole, a sudden change in temperature is observed.

328

329 The flow of fluid at the estimated rates of 0.4 – 0.04 ml/s in the 22 cm diameter

330 Outokumpu hole would generate temperature anomalies (jumps) smaller than 2 mK

331 (Drury, 1984; eq. 1-3) at the in/outflow depths. In order to detect the flow in

332 temperature logs would require anomalies clearly exceeding the temperature

333 resolution (0.01 K). This would mean flow rates of the order of 4 ml/s which would

334 generate temperature effects of about 0.02 K. Such anomalies could be detected in
335 principle. However, the flow rate of 4 ml/s would be in contradiction with the slow
336 time-dependent changes in fluid salinity.

337

338 At the depths of the major in/outflow indicated by the fluid electrical conductivity
339 logs (Fig. 5) we do not observe any distinct changes in the temperature logs. The
340 calculated gradient logs, on the other hand, seem to show local maxima and minima at
341 about 230 m, 950-1,000 m, 1,700-1,750 m, 2,250 m, 2,300 m, and 2,430 m (Fig. 6),
342 which may be attributed to flow effects. In addition, the gradient changes do not seem
343 to correlate with local conductivity variations at these depths.

344

345 We conclude that although minor flow systems exist in the hole, they are driven by
346 the density differences due to replacement of fresh drill hole water by saline formation
347 fluids. The flow does not have any relevant effects on the thermal data. The same
348 applies to the effects of free thermal convection of the drill hole fluid (see discussion
349 below).

350

351 *Flow in the formation* is theoretically possible, but flow systems able to generate the
352 detected vertical heat flow variation are not likely. In an earlier study, possible
353 advective heat transfer effects were estimated for a similar type of a structure in
354 Sukkulansalo located in the Outokumpu belt at a distance of about 20 km NE from the
355 deep hole (Kukkonen and Šafanda, 1996). Hydraulic *in situ* permeabilities of the rock
356 types measured in the uppermost 1 km were in the range of $1 \cdot 10^{-17} – 1 \cdot 10^{-16}$ m^2 for
357 mica gneiss, serpentinite, skarn rock and talc schist, and in the range of $1 \cdot 10^{-14} – 1$
358 $\cdot 10^{-15}$ m^2 for black schist (Ahonen et al., 1991; Ahonen and Blomqvist, 1994). Mainly
359 due to the small topographic variation, and low hydraulic conductivities of the rock,
360 the Peclet numbers of advective heat transfer estimated and modelled by Kukkonen
361 and Šafanda (1996) with 2D analytical and numerical models were of the order of 10^{-4}
362 $– 10^{-5}$. In the Outokumpu deep hole, drill stem tests were carried out during drilling
363 breaks after each 500 m of drilling in 40 – 70 m long test sections at hole bottom
364 (Ahonen et al., 2011). The results indicated a relatively high value ($0.7 \cdot 10^{-12}$ m^2) at
365 480 – 580 m and a moderate value ($5 \cdot 10^{-14}$ m^2) at 957-997 m, whereas all deeper test
366 sections were observed to be practically impermeable. A quantitative limit of
367 impermeability is not given by Ahonen et al. (op. cit.), but is likely around 10^{-16} - 10$^-$

368   ^{17} m^2 in the applied test method. Unfortunately, the drill stem tests do not provide a
369   continuous profile of permeability data with depth, and furthermore, the two
370   uppermost test sections coincide with well-developed fracture systems detected in the
371   drill core as well as in galvanic, sonic and calliper logs (Ahonen et al., 2011;
372   Tarvainen 2006, Fig. 5). Thus, these values probably overestimate the permeability of
373   the formation. Anyway, the results imply a rapidly decreasing permeability with depth
374   in the deep hole. In the uppermost 200 m fracturing is common in the deep hole (Fig.
375   5).

376

377   The possible contribution of advection was estimated with dimensional Peclet number
378   analysis (van der Kamp and Bachu, 1989; see also Kukkonen, 1995 for application of
379   the method in Finnish conditions) assuming a hydraulic gradient of $4 \cdot 10^{-3}$ determined
380   from local topography and lake levels in a NW-SE profile across the deep hole site.
381   The Peclet number (*Pe*) gives the ratio of heat transported by advection to that
382   transported by conduction and can be calculated as (van der Kamp and Bachu, 1989):

383

384   $$Pe = \beta \kappa \frac{dh}{dl} DA / \alpha_m \qquad (1),$$

385

386   where *β* is the ratio of volumetric heat capacities of the fluid and the medium (about
387   1.83), *κ* is the hydraulic conductivity, *dh/dl* is the hydraulic gradient, *D* is the
388   thickness of the aquifer, *A* is the aspect ratio of the aquifer (*A* = *D/L*, where *L* is
389   length), and α_m is the diffusivity of the medium (about $1 \cdot 10^{-6}$ m^{2}s^{-1}). Peclet number
390   values exceeding about 0.1-0.2 would indicate a detectable level of advective heat
391   transfer. Assuming that the flow system (i.e., permeable rock) in Outokumpu would
392   extend to a depth of 1 km and the flow distance were 10 km, the Peclet number
393   reaches a value of 0.1 only if permeability exceeds $1.5 \cdot 10^{-13}$ m^2. However, we do not
394   consider such permeability values representative of the rocks in the Outokumpu belt.
395   The chances of advective heat transfer effects in the formation are further reduced by
396   the overall increase of fluid salinity (and density) with depth which tends to debilitate
397   any potential flow systems. The heat transfer is therefore dominated by conduction.
398   Similar results on advective heat transfer contribution were obtained by running
399   coupled finite difference conductive-advective heat and fluid flow models (results not
400   shown here).

401

402

6. Free convection of fluid in the borehole

404

405   When pulling out the memory-logger temperature probe from the hole in August
406   2005, it got temporarily stuck at the depth of 1390 m. The probe (resolution 1 mK,
407   manufactured by Antares GmbH, Germany) continued logging temperatures for
408   several days thereafter until the memory was full. Due to this incident, we obtained a
409   high-resolution time series of temperature (Figure 7), which clearly evidences
410   continuous temperature variations with amplitude of few mK taking place in periods
411   ranging from minutes to several hours. Instrument noise can be excluded as a reason
412   for the variations and they must be attributed to natural phenomena in the borehole.
413   Time dependent variations in borehole water table (and therefore temperatures
414   recorded by a stationary probe) can be generated by several factors, namely tidal
415   effects (Bredehoeft, 1967; Hsieh et al., 1987; Cutillo and Bredehoeft, 2010),
416   barometric pressure variations (Spane, 2002) and free convection of fluid in the
417   borehole (Hales, 1937; Čermak, 2009, Čermak et al., 2008a,b,c; Eppelbaum and
418   Kutasov, 2011). The deep hole water table is automatically monitored with a pressure
419   sensor at 20 m depth. In addition the water table is monitored in a 17 m deep well in
420   the Quaternary sandy-silty sediments located at about 20 m from the deep hole.
421   Atmospheric pressure is also monitored on the site (Hänninen et al., 2009). The water
422   table variations in the deep hole and the shallow hole are not correlated which
423   indicates that the shallow Quaternary aquifer is not hydraulically connected to the
424   deep hole.

425

426   Tidal effects are present in the deep hole water table variations. Spectral analysis of
427   data obtained (during a technically quiet period with no logging or fluid pumping
428   activities) between Nov 11, 2007 and April 17, 2008 with 30 min recording intervals
429   shows distinct periodicities at frequencies 1.00, 0.93, 1.93 and 2.00 cpd (cycles per
430   day). They correspond accurately with the lunar-solar, principal lunar and principal
431   solar tidal components (Munk and MacDonald, 1960). Groundwater table variations
432   corrected for atmospheric pressure variations show peak-to-peak amplitude of 2-6 cm
433   (Hänninen et al., 2009). Corresponding movement of the water column in the
434   borehole can be expected to generate temperature variations smaller than 1 mK.

435

436 Barometric effects also generate water table variations (Spane, 2002). As they are

437 driven by meteorological phenomena their characteristic periodicities are about one

438 order of magnitude longer than the recorded temperature variations. As the tidal and

439 barometric pressure effects do not explain the temperature variations, we investigate

440 the possibility for free convection.

441

442 Based on our former experience (Čermak et al., 2008a, b) free convection is indeed

443 present in large diameter boreholes. When a long fluid-filled column is subjected to a

444 thermal gradient, free thermal convection may occur as soon as the temperature

445 gradient exceeds a certain critical value. Such borehole fluid instability was originally

446 described and theoretically treated by e.g. Hales (1937) and reported to exist only in

447 large diameter wells.

448

449 The onset of free convection depends mainly on the borehole diameter and

450 temperature gradient. The critical temperature gradient value G_c, above which

451 convection takes place (Hales, 1937), can be calculated from

452

453 $$G_c = \frac{g\alpha T}{C_f} + \frac{16B\nu k}{g\alpha d^4}$$ (2)

454

455 where g is the acceleration of gravity, T is absolute temperature, α is the coefficient of

456 thermal expansion, k is the diffusivity, ν the kinematic viscosity, C_f is the specific heat

457 of fluid (4183 J K^{-1} kg^{-1} for water at 20°C), and B is a constant which has the value

458 216 for a tube whose length is great compared with its diameter (d). For the

459 Outokumpu hole (diameter 22 cm) the critical gradient is about 0.3 mK/m, which is

460 about fifty times smaller than the measured geothermal gradient values. Therefore,

461 free convection very probably takes place and the Outokumpu monitoring data

462 supports this conclusion. The measured data reveals a complex stochastic structure of

463 the microtemperature field. In analogy to the previous results based on theoretical

464 considerations discussed in previous experiments (Čermak et al., 2008c) the height of

465 convection cells is probably of the same order of size as the hole diameter; the

466 characteristic period of the process amounts to 2.5-2.8 hours. This is in good

467 agreement with the weak periodicities observed in the temperature data. Although the

468   borehole fluid becomes more saline and denser with increasing depth, the fluid

469   density is practically constant over distances of convection cell heights. Therefore the

470   fluid salinity has no effect on such small scale convection.

471

472   The free convection creates only local temperature variations, which do not jeopardize

473   the overall geothermal results. However, it generates a certain background "noise"

474   level that limits the temperature resolution that can be achieved in studying local

475   temperature variations in a large diameter hole.

476

477   **7. Palaeoclimatic effects: Forward and inverse transient heat transfer models**

478

479   *Forward modelling.* As there is no significant topography in the Outokumpu area, and

480   the hydraulic conductivities (Tarvainen, 2006; Ahonen et al., 2011) are relatively low,

481   forced convective heat transfer probably does not play a role in the vertical

482   temperature gradient and heat flow variations. Therefore, the general vertical gradient

483   variation is most probably due to palaeoclimatic ground temperature variations on the

484   Outokumpu drilling site, but probably also affected by structural effects (i.e.,

485   conductivity and heat production). We have used the latest temperature log

486   (September 2008) for forward and inverse modelling of the ground surface

487   temperature (GST) history.

488

489   The forward modelling was done in 2D with a finite difference modelling code

490   Processing Shemat (Clauser, 2003) and the model structure was constructed using

491   reflection seismic data (Kukkonen et al., 2006, see Fig. 3). The model size is 10 km x

492   10 km (Fig.8) and the basic discretization is 100 m x 100 m, but locally refined in the

493   uppermost parts model and in the vicinity of the deep hole to 10-50 m cell size.

494   Applied thermal parameter values are shown in Table 2. For volumetric heat capacity

495   the average of $1.88 \cdot 10^6$ J m^{-3}K^{-1} of the deep hole rocks was used. As the porosity of

496   crystalline rocks is very small (<0.5%) we ignored the latent heat of freezing and

497   thawing pore water. The GST variation was modified step by step until a satisfactory

498   agreement with measured temperatures was achieved. Here we could use the earlier

499   results by Kukkonen and Šafanda (1996) as first approximations of a possible GST

500   history in the Outokumpu area. A measure of the two-dimensionality of the modelled

501   structure is provided by the simulated vertical and horizontal components of heat flow

502   density. 2D thermal conductivity contrasts affect the heat flow vector and deflect it

503   from the vertical due to channelling (or refraction) of heat flow to inclined high

504   conductivity layers. Our thermal model suggests that the horizontal components of

505   heat flow in the deep hole section are very local and smaller than 2 mW m^{-2} which is

506   equivalent to a deviation of the heat flow vector by less than 4 degrees from vertical.

507   This is due to the relatively small dips of the rock type layers (Fig. 8), which strongly

508   constrain the refraction effects. It means that a 1D approximation could also be

509   applied, which was actually done in the inverse modelling below.

510

511   In our final transient 2D model (Fig. 9) the Weichselian was preceded by a steady-

512   state with GST of 5°C, and during the Weichselian temperature is assumed to be -3 °C

513   between 91 ka BP and 9 ka BP. During the subsequent "Holocene optimum" GST was

514   7°C, decreasing to 6°C at 5000 BP, further to to 4.6 °C at 800 BP and finally

515   increasing to 5.2°C at 300 BP which was kept until the present.

516

517   The modeling is quite sensitive for the basal heat flow (in the final model 20.5 mWm^{-2}

518   at 10 km). Changing the basal heat flow by 0.5 mW m^{-2} affects the temperature at

519   2.5 km by about 0.3 degrees. The Outokumpu data is not simple to fit with a GST

520   history. This is due to a relatively constant gradient down to about 1.3 km. To

521   simulate this we need downward diffusing GST signals which compensate each other.

522   Anyway, it is possible to find a GST history which works with the measured data and

523   includes the main components of Holocene climate history (Fig. 9). The temperature

524   fit is mostly within ±0.1…0.2 K. Respectively, the simulated heat flow values (Fig.

525   11) are in a good agreement with values measured in the deep hole (Fig.6).

526

527   *Inverse modelling.* 1D inversions were performed with the smooth Tikhonov-type

528   inversions described by (Rath and Mottaghy, 2007). For this purpose, a numerical

529   model was constructed down to a depth of 5000 m. For this, logarithmic spatial and

530   temporal meshes were used, with 700 and 600 cells respectively. This logarithmic set

531   up was found to be advantageous when modelling the propagation of a broad-band

532   GSTH signal into the earth.

533

534   In order to associate temperatures and rock properties to grid cells, both temperature

535   and the measured rock thermal conductivities had to be upscaled. For thermal

536 conductivities this was accomplished by using the weighted harmonic mean of all

537 measured values in a cell, assuming dominantly vertical heat conduction.

538 Temperature, however, is available at a higher sampling rate (0.1 m). Therefore we

539 chose a smoothing interpolation of temperatures for each cell (Garcia 2010), where

540 the smoothing parameter was determined by Genaralized Cross Validation (Wahba

541 1990). Residuals between observed and interpolated temperatures are shown in Figure

542 12. As the residuals show a reasonably Gaussian distribution, we believe that the bias

543 introduced by the upscaling procedure is small compared to other sources of error.

544 The harmonic mean is less sensitive to high conductivities (say, > 6 $Wm^{-1}K^{-1}$), which

545 fortunately constitute only a very small fraction (<1%). Thermal diffusivity was

546 estimated from conductivity based on the petrophysical studies which support a linear

547 dependence (*s $[10^{-6} m^2 s^{-1}]= 0.503 \lambda + 0.0839, R^2 = 0.94$*).

548

549 The model assumes a 1D layered structure with conductivity and heat production in

550 the uppermost 2.5 km as determined from logs and laboratory measurements in the

551 deep hole. Between at 2.5 – 5 km, a constant thermal conductivity of 2.9 $Wm^{-1}K^{-1}$

552 was assumed. For heat production, a value between pegmatite and metamorphites was

553 obtained by multiplying the value for the pegmatites (H in Fig. 13) by a factor of 0.8,

554 roughly corresponding to the proportions of pegmatites and metamorphites. The

555 values of λ and heat production are somewhat arbitrary, because for this 1D model the

556 conditions below 2500 m the borehole only add to the heat flow density at the bottom

557 of the hole, equivalent to changing the (fictious) value of heat flow density a 5000 m.

558

559 GSTH war parametrized by a logarithmically spaced series of step functions, between

560 100 kyrs b.p. and 10 yrs b.p., in order to take care of the decreasing resolution with

561 depth. As is well known, GSTH inversion is an ill-posed problem. Regularization was

562 done by a combination of zero and first order derivative matrices (see Rath and

563 Mottaghy, 2007; Aster et al., 2005). Instead of adapting sophisticated methods of

564 determining the regularization parameters, a simple decreasing schedule was adopted,

565 starting with predetermined values and reducing them by a fixed factor at each

566 iteration, until a target misfit is reached (see e.g., Newman and Hoversten 2000). For

567 all inversions, a constant prior corresponding to the current surface temperature of 5

568 ºC was assumed.

569

570 Inversion results thus obtained (Fig. 13) suggest the following: Nearly independent of

571 the parameterization chosen, a rather stable GSTH for the last few thousand years was

572 found. In particular, the results for the last two millenia are insensitive to the choice of

573 the basal heat flow. In most cases, a reasonable fit could be found for depths <1500

574 m, with $|T_{obs} - T_{mod}| < 0.1$ K for the top 1000 m, and < 0.2 K for $z < 1500$ m. As the

575 influence of the post-glacial warming can be approximated by a linear trend (or biased

576 heat flow) for short boreholes (Rath et al., 2010), it could be interpreted that the

577 results are not biased by non-stationary conditions and may be interpreted

578 independently. Temperatures of the LGM, however, are sensitive to the assumed heat

579 flow density and heat production. Moreover, the data fit deteriorates strongly below

580 1500 m. Here, the residuals increase up to ±0.3 K even for the best cases. This is

581 probably due to different effects: (1) Fluid inflow may be important for depths > 1500

582 m (see Fig. 5), (2) heterogeneity effects may produce temperature distributions not

583 consistent with 1D conditions, and (3) there may be a residual contribution of post-

584 drilling equilibration of temperatures. All these effects are not easily coped with in the

585 framework of 1D inversion, and must be left to future studies.

586

587 Systematic variation of basal heat flow and pegmatite heat production show that a

588 similar fit can be obtained for many combinations of these two parameters. Plotting

589 inverted models for parameter combinations along this elongated minimum of

590 residual norms reveals that all these GSTHs are very similar. Figure 14 shows

591 contours of the

592 $$RMS = \sqrt{N^{-1} \sum \sigma_i^{-1} \left(T_{i,obs} - T_{i,calc} \right)^2} \qquad (3),$$

593 and the GSTHs corresponding to the minimum. These results are very similar for

594 basal HFD between 26 and 36 mWm^{-2} and pegmatite heat productions between 1

595 and 6 μWm^{-2} , showing a high degree of equivalence in the model. However, all

596 these GSTHs produce practically the same fit (RMS≈0.9).

597

598

599 A tentative interpretation of the reasonably well-resolved part of the GSTH can be

600 given. The minimal temperatures for the LGM were 7 to 9 K lower than today, i.e.

601 between -2 and -4 ºC. Mainly due to the problems originating from the effect

602   mentioned above, the post-glacial temperature rise is too smooth, as in this case the

603   inversion is dominated by the smoothing regularization method. Generally, a warm

604   Holocene (anomaly 2-3 K) was found, reaching its maximum near 4 kyrs b. p.,

605   broadly consistent with regional proxy reconstructions. There is no signature of a

606   Medieval Warm Period, and the Little Ice Age appears rather flat with no clear

607   indication of distinct minima. Finally, a strong recent warming of about 0.5 K is

608   visible in the last 50 years. In comparing the present results with various

609   palaeotemperature histories derived from proxies and meteororological data which

610   commonly refer to the air temperature, we have to take into account that ground

611   surface temperature in Finland is 1-2 K higher than air temperature (Kukkonen, 1987;

612   linear dependence for annual average temperatures: *T(ground) (°C) = 0.71 T(air) +*

613   *2.93*). The difference is due to the insulating effect of the winter snow cover. Thus,

614   the behavior observed in the inversion results is generally consistent with various

615   proxy reconstructions given in Seppä & Poska (2004), Heikkilä & Seppä (2003), and

616   Luterbacher et al. (2004).

617

618   During the 20th century the drilling site likely experienced several changes in the

619   vegetation cover due to the Outokumpu town which started to grow quickly after the

620   discovery of the ore deposit in 1910. Therefore, there have been significant changes in

621   the environment due to clear cutting of forest and building of the railroad to the S side

622   of the drilling site, and the warming trend of the last 50 years may be partly related to

623   man-made effects. The present forest surrounding the site is about 30-50 years old and

624   it was most probably clear-cut before that. The drilling site (area 0.6 ha) was clear-cut

625   in the forest and covered with gravel in 2003. This removal of the vegetation is clearly

626   reflected in the temperature curves in the uppermost 50 m.

627

628   **8. Discussion**

629

630   The geothermal results of the Outokumpu deep drill hole indicate that there is a

631   distinct vertical variation in temperature gradient and heat flow density. Due to the

632   high resolution of data obtained both in the drill hole logging as well as in laboratory

633   measurements, the conductivity, gradient and heat flow values could be determined

634   with very small determination errors (Table 2). The measured heat flow data in the

635   uppermost 1 km differ by about 10 mW m^{-2} from the undisturbed values (about 42

636   mW m^{-2}, Fig.11). The difference is significant and must be taken into account in
637   applying heat flow data for estimating temperatures deeper in the crust. The result is
638   in good agreement with the average vertical variation in heat flow density in
639   Fennoscandia and the East European Platform (Kukkonen and Jõeleht, 2003). The
640   vertical variation in heat flow density in the Outokumpu deep hole is very likely due
641   to palaeoclimatic GST variations during the last 100,000 years. Structural effects,
642   such as refraction of heat can be excluded, because the subhorizontal dip angles of the
643   lithological contacts attenuate the effects of heat flow refraction to insignificant.
644   Correspondingly, heat transfer by advection is also considered to be negligible.

645

646   The result has important implications for analysing and correcting heat flow data in
647   the Fennoscandian Shield (c.f., Majorowicz & Wybraniec, 2010). The need of
648   correcting heat flow data for palaeoclimatic effects has been known for a long time
649   (e.g. Birch, 1948; Jessop, 1971; Beck, 1977), but the problem is that usually the GST
650   history is not known sufficiently accurately to allow reliable forward corrections, and
651   shallow holes (< 1 km) do not provide unique solutions for the long-term climatic
652   GST variations, but ignoring them, especially the glaciations, will bias the heat flow
653   values significantly.

654

655   Earlier palaeoclimatic corrections for Weichselian and Holocene effects in heat flow
656   values from about 1 km deep holes in the Outokumpu belt have given values of 6 - 7
657   mWm^{-2} (Kukkonen, 1987, 1989). These corrections assumed that the Weichselian
658   GST was at the pressure melting temperature of a thick ice sheet, i.e. about -1°C.
659   Kukkonen and Šafanda (1996) modelled the GST history in the Outokumpu belt
660   (holes about 1 km deep) with forward modelling and obtained an estimate of -2°C for
661   the Weichselian GST. The present forward and inverse results suggest -3°C for the
662   Weichselian GST and the correction for palaeoclimatic effects is about 10 mWm^{-2} for
663   the average heat flow value in the uppermost 1 km. Our result suggests a correction
664   smaller than the one applied by Majorowicz & Wybraniec (2010) for northern Europe.
665   Their correction is +19 mWm^{-2} at surface and about 16 mWm^{-2} for an average
666   correction in the uppermost 1 km, and the corrected heat flow value for eastern
667   Finland is given as about 50 mWm^{-2} which is considerably higher than our present
668   Outokumpu result of 42 mW m^{-2}. The difference is due to the much higher glacial-
669   interglacial GST difference applied (14 K) and that Holocene effects were not

670   included in the correction of Majorowicz & Wybraniec (2010). The Holocene effects,

671   particularly the relatively long HCO warm period, would tend to reduce the overall

672   correction in the uppermost 600 m. On the other hand, Slagstad et al. (2009) used a

673   palaeoclimatic correction for the Fennoscandian area assuming glacier basal

674   temperatures as -1°C resulting in somewhat smaller corrections than the Outokumpu

675   data suggest. The Outokumpu results emphasize the importance of experimental

676   results from deep boreholes in constraining the necessary corrections of geothermal

677   data.

678

679   Very low apparent heat flow values (2-12 mW m^{-2}) were reported in eastern Karelia,

680   Russia, by Kukkonen et al. (1998) in a number of holes <750 m deep. The study site

681   is located about 350 km to the E of Outokumpu. Advective fluid heat transfer and

682   structural factors could be excluded and the low heat flow values were attributed to

683   low Weichselian GST as low as -10…-15°C. The area was outside the Weichselian

684   ice sheet for most of time and therefore experienced periglacial low temperatures. If

685   the indicated GST values are representative they would imply a considerable

686   difference in Weichselian GST values between Outokumpu and eastern Karelia.

687

688   The Outokumpu area was covered by ice sheets perhaps only during the Middle

689   Weichselian (about 60,000 years B.P.) and Late Weichselian (about 20,000 years

690   B.P.) glacial maxima (cf. Hubberten et al., 2004; Svendsen et al., 1999, 2004).

691   Radiocarbon dating of mammoth fossils suggests that most of southeastern

692   Fennoscandia (and Outokumpu) was probably ice-free during 37,000 – 26,000 years

693   B.P. (Ukkonen, et al., 1999; Lunkka et al., 2001). The isotopic composition of oxygen

694   in woolly mammoth teeth enamel can be used as a proxy for palaeotemperatures, and

695   it yields annual mean surface proxies in the range of -1 ... -3 °C in southern and

696   central Finland and NE Russia for Middle Weichselian (about 52,000 – 24,000 years

697   B.P.) (Arppe and Karhu, 2006, 2010). The paleotemperatures obtained from

698   mammoth fossils are in a good agreement with the Outokumpu geothermal result on

699   Weichselian average GST.

700

701   When interpreting the geothermally derived GST values in terms of paleoclimate, it

702   should also be kept in mind that the basal temperatures of a glacier are usually not

703   spatially or temporally constant. The GST under a thick ice sheet with basal pressure

704 melting (about -1 °C) can actually be higher than the GST in surrounding ice-free

705 areas experiencing very cold periglacial climate (Paterson, 1994). On the other hand,

706 areas under the ice divide where downward advection of ice dominate, may have

707 basal temperatures well below freezing (e.g. in the Greenland ice sheet; Dahl-Jensen

708 et al., 1998).

709

710 The forward and inverse modelling of the GST history suggests that the surface was

711 about 8 K below present during the cold Weichselian climatic period (GST -3…-4°C).

712 The downward attenuated GST signal does not provide high resolution for the Middle

713 and Early Weichselian in a 2.5 km deep hole, and no details can be provided for these

714 periods, although the inverse modelling (Fig. 13) could suggest trends there, too. The

715 solution is, however, non-unique and depends on the deep heat flow value and the

716 heat production at depths beneath the deep hole bottom. Selecting the heat flow and

717 heat production values yielding the smallest RMS values in inversion the obtained

718 GST history becomes very stable and suggests surface temperatures of -3…-4 °C

719 during the Weichselian (Fig. 14). Due to poor temporal resolution of the temperature

720 history during the Weichselian the GST value should be regarded as an estimate of the

721 average value.

722

723 The transient modeling provides also an estimate of the permafrost thickness in

724 Outokumpu, which had maximum at the end of the cold Weichselian period. The

725 forward model indicates that permafrost would have extended to about 150 m at the

726 Weichselian-Holocene transition at about 9,000 years B.P. We can compare this result

727 with other logging and core data and speculate that the maximum depth reached by

728 permafrost would be reflected in the fracture frequency in the uppermost parts of the

729 hole. Freezing of pore and fracture water causes cracking and opening of existing

730 fractures, which would gradually increase the fracture volume in each permafrost

731 cycle. The hydraulically conductive fractures interpreted by Tarvainen (2006) from

732 the density, acoustic and galvanic down-hole logs are much more frequent in the

733 uppermost 200-300 m than in deeper levels (Fig. 5). The near-surface fracturing is

734 naturally contributed by other factors than only permafrost, such as slow relaxation of

735 lithostatic pressure by erosion and weathering, but freeze cracking by permafrost is a

736 conceivable process in the origin of the near-surface fracturing. Fracturing may also

737 have been inherited from other earlier Quaternary cold climatic periods than only the

738 Weichselian.

739

740 The small temperature gradient and heat flow variations in the uppermost 1 km

741 requires that the Holocene variations in GST were within ±2 K from the present GST

742 value. The Holocene GST history obtained by the smooth inversion (Fig. 13) is a very

743 stable result particularly for the latest 2,000 years which are not affected by

744 uncertainties in the deep heat flow or heat production. The Holocene Climatic

745 Optimum (HCO) is shifted towards more recent times in our result than conventional

746 palaeoclimatic proxy data suggest and the maximum is seen around 4,000 years B.P.

747 The result differs from typical Holocene temperature reconstructions, and e.g. proxies

748 from pollen stratigraphy in southern Finland (Heikkilä and Seppä, 2003) show that the

749 HCO temperature was at maximum about 6,000 years B.P. This reflects the problems

750 with the regularization parameters in the inversion which smoothes the very strong

751 and steep signal of the Weichselian-Holocene transition and spreads it apparently to

752 Early Holocene. The results for later times show only weak variations. Moreover, the

753 temperatures obtained are approx. 2 K higher than paleotemperature reconstructions

754 from nearby points as in Heikkilä and Seppä (2003), Seppä and Poska (2004) or

755 Luterbacher et al. (2004). This reflects the difference between ground and air

756 tempertures, as discussed above, and the distances between proxy study sites and

757 Outokumpu. In Fig. 13 we also have plotted the European temperature reconstruction

758 for the last 500 years, which were interpolated to the geographical coordinates of

759 Outokumpu. Our results fit the general behaviour quite well. However, there is larger

760 disgreement in the last hundred years, which cloud be due to the history of land use

761 change and deforestation in the industrial age. This is speculative, but deserves further

762 investigations.

763

764 Assuming that the geological structure can be approximated as a 1D horizontally

765 layered structure, and that heat transfer is conductive, Fourier's first law of heat

766 conduction (i.e., heat flow density = conductivity x gradient) is in force. Therefore,

767 thermal conductivity and measured temperature gradient should be inversely

768 correlated. However, the simple inverse relationship is affected by transient effects

769 (palaeoclimate) and heat production, and therefore it is not expected to hold in

770 absolute values of conductivity and gradient in the scale of the complete borehole.

771 Nevertheless, the inverse relationship can be assumed to exist locally representing
772 small scale variations (in the scale of 10-100 m). Such a relationship is indeed
773 observed in the Outokumpu hole data. It holds particularly in depth sections where
774 there are strong thermal conductivity contrasts, such as (1) between the ophiolitic
775 rocks and surrounding mica schist, (2) between serpentinites and skarn within the
776 Outokumpu rock type assemblage, as well as (3) between the pegmatitic granite and
777 mica schist (Fig. 6). The relationship is however, not completely systematic, and
778 deviations can be seen in the upper parts of the hole. They may reflect small scale
779 heterogeneities which are not sufficiently 1-dimensional, or alternatively small fluid
780 flow effects. For instance, at the depth of 230 m there is one of the hydraulically
781 active fractures interpreted to cause flow out from the hole (Fig. 5) and the
782 conductivity variations do not seem to correlate with gradient over the 200-300 m
783 interval.

784

785 Heat transfer is dominantly conductive in the deep hole structure. This is
786 demonstrated by the lack of thermally relevant fluid flow effects between fractures
787 and the hole, as well as the inverse correlation of gradient and conductivity.
788 Moreover, the low hydraulic conductivity of the crystalline rocks in general (Clauser,
789 1992; Manning and Ingebritsen, 1999), and in the Outokumpu area (Kukkonen and
790 Šafanda, 1996; Tarvainen, 2006; Ahonen, 1991; Ahonen and Blomqvist, 1994;
791 Ahonen et al., 2011) together with the small topographic hydraulic gradients suggest
792 that the magnitude of heat transfer by fluid flow in the formation, if present, is very
793 probably negligible. The downward increasing fluid salinity (and thus density) further
794 tends to attenuate flow systems. In Outokumpu, the saline fluids recovered from the
795 open borehole as well as pumped from fractures isolated by hydraulic packers also
796 show vertical variation in their chemical composition (Ahonen et al., 2011). It speaks
797 for minimal mixing and long residence times of groundwater in the fractured medium
798 penetrated by the drill. Conductive heat transfer very likely dominates over advection.
799

800 During the Weichselian glaciation, the subglacial hydrogeological conditions may
801 have resulted in significant recharge of glacial meltwater into the bedrock which may
802 have produced advective heat transfer still affecting the present temperatures.
803 Theoretical modelings and experimental data on subglacial hydrology and
804 groundwater flow (Boulton et al., 1995, 1996; Person et al., 2007; Lemieux et al.,

805   2008; Lemieux and Sudicky, 2010) have suggested that in northern Europe and North

806   America considerable recharging of glacial melt water took place under the

807   Weichselian and Laurentian ice sheets. In Canada, the recharge depth may have

808   extended up to 2 - 3 km. The glacial hydrology may have considerably altered the

809   groundwater flow systems, flow directions and affected the groundwater chemistry,

810   particularly in the aquifers in sedimentary rocks, but also in crystalline shield rocks.

811   These results depend strongly on the subglacial hydraulic heads and hydraulic

812   conductivity of the bedrock and are therefore dependent on rock types, fracturing and

813   local glacial conditions. The existence of eskers in the shield areas glaciated during

814   the Weichselian glaciation in northern Europe is attributed to channelling of

815   subgalcial meltwaters at the interface between ice and low-permeability bedrock. On

816   the other hand, there are no or only rare eskers in areas of sedimentary rocks which is

817   attributed to the recharging of meltwaters into the permeable sedimentary rocks and

818   aquifers in them (Boulton et al., 1995, 1996, 2009; Vaikmäe et al., 2001; Jansson et

819   al., 2007; Jansson 2010).

820

821   The order of magnitude of the thermal effect of the recharge can be estimated from

822   the infiltration rates of meltwater into bedrock during the glaciation. The infiltration

823   rates are not simple to estimate, but some values are available. Person et al. (2007)

824   estimate from geochemical and environmental isotopic data that the volume of

825   recharged meltwater in sedimentary rock aquifers in North America may amount up

826   to 0.2 – 10 % of the total amount of meltwater. Lemieux et al (2008) estimated that

827   the subglacial infiltration rate was on the average about 2 mm/yr in the Canadian

828   Shield area during the Wisconsinian glaciation. Using the value by Lemieux et al.

829   (2008) the corresponding Peclet number for vertical (1-D) filtration of water in a

830   permeable layer can be calculated as (Bredehoeft and Papadopoulos, 1965):

831

832    $Pe = V_D \rho_f C_f L / K$ (4),

833

834   where V_D is the recharge flux (Darcy velocity), ρ_f is fluid density, C_f is fluid specific

835   heat capacity, L is layer thickness and K is thermal conductivity. Assuming that the

836   hydraulically permeable zone was 1-2 km thick in Outokumpu during glaciation and

837   rock thermal conductivity is 2.5 $Wm^{-1}K^{-1}$, the (steady-state) Peclet number would be

838 about 0.1 - 0.2. Such a disturbance in heat flow would be a small one, but possibly

839 detectable under favourable conditions. However, the limited duration of ice cover

840 (approximately 5,000 – 10,000 yr during each glacial) and the fact that glaciation (and

841 the infiltration) ended already about 10,000 yr ago result in further reduction in the

842 subglacial advective heat transfer effects on the present heat flow. It is possible that

843 traces of a small advective palaeohydrological heat transfer component could be

844 present in the Outokumpu temperature data, but the effect is very small and would be

845 very difficult to distinguish from transient conductive effects by palaeoclimatic GST

846 variations. We note that the subglacial hydrogeology of the Weichselian ice sheet

847 would need more attention in future studies to allow more accurate estimation of the

848 possible advective heat transfer effects by subglacial groundwater flow.

849

850 The critical gradient for the onset of free convection of fluid in the borehole is clearly

851 exceeded in the Outokumpu hole, and convection was experimentally confirmed with

852 time-dependent temperature records. The free convection is sluggish and generates

853 time-dependent temperature variations with a maximum amplitude of about 0.01 K,

854 and the convection cells are about as tall as the hole diameter (0.22 m). In single logs

855 obtained with temperature resolution of 0.01 K at logging speeds of about 5-10 m/min

856 and with reading intervals of 0.1-0.2 m, free convection can be expected to show as

857 single anomalous readings which cannot be easily separated from instrumental noise.

858 Moreover, the temperature variations are smoothed by the convolution of the

859 temperature-depth profile depending on the time-constant of the logging tool and the

860 applied logging speed in continuous loggings. As a result, we consider the free

861 convection as a source of thermal noise, which does not harm the overall results or

862 modeling.

863

864

865 **9. Conclusions**

866

867 The geothermal studies in the Outokumpu deep drill hole revealed a distinct vertical

868 variation in heat flow density. Heat flow density increases from about 28-32 mW m^{-2}

869 in the uppermost 1000 m to 40-45 mW m^{-2} at depths exceeding 2000 m. The vertical

870 variation can be attributed mostly to the cold climatic Weichselian period (about

871 91,000 – 9,000 years B.P.). The forward and inverse modelling suggests that the GST

872 was about -3...-4°C during Weichselian time. Inversion for Holocene GST history
873 yields a relatively stable GST within ±2 K from the present value (5°C). The
874 Outokumpu results further suggest that the correction for palaeoclimatic effects in
875 heat flow data measured in the uppermost 1 km in eastern Finland should be about 10
876 mWm^{-2}. Heat transfer in the Outokumpu section is dominated by conduction and no
877 relevant advective heat transfer effects by groundwater flow could be observed. In the
878 hole, minor effects of fluid flow between fractures and the hole can be observed,
879 which we attribute to replacement of fresh drilling fluid with saline formation fluids.
880 Free convection takes place in the borehole and can be detected with very sensitive
881 temperature recordings, but the convection produces temperature variation with very
882 small amplitudes which can be treated as a source of thermal noise not affecting the
883 heat flow results or modelings.

884

885 *Acknowledgements*

886

897
898

References:

Ahonen, L., Blomqvist, R., Kurimo, M., Kuivamäki, A., 1991. Kalliopohjavesiolosuhteet Outokummun Sukkulansalossa: Vuoden 1990 tutkimukset (Deep bedrock hydrogeological condition in the Sukkulansalo area, Outokumpu: Results of 1990). Geological Survey of Finland, Nuclear Waste Disposal Research, Report YST-75, 42 pp. (in Finnish with English abstract)

Ahonen, L. and Blomqvist, R., 1994. Mode of occurrence of deep saline groundwater in Finland based on hydraulic measurements. In: B. Olofsson (ed.), *Salt groundwater in the Nordic countries*, Research Council of Norway, Oslo, NHP Report, 35, 49-59.

Ahonen, L., Kietäväinen, R., Kortelainen, N., Kukkonen, I.T., Pullinen, A., Toppi, T., Bomberg, M., Itävaara, M., Nousiainen, A., Nyyssönen, M., Öster, M., 2011. Hydrogeological characteristics of the Outokumpu Deep Drill Hole. In: I.T. Kukkonen (ed.), Outokumpu Deep Drilling Project 2003-2010, Geological Survey of Finland, Special Paper, 51, 151-168.

Arppe, L.M., Karhu, J.A., 2006. Implications for the Late Pleistocene climate in Finland and adjacent areas from the isotopic composition of mammoth skeletal remains. Palaeogeogr. Palaeoclim. Palaeoecol., 231, 322-330.

Arppe, L.M., Karhu, J.A., 2010. Oxygen isotope values of precipitation and the thermal climate in Europe during the middle to late Weichselian ice age. Quat. Sci. Rev., 29, 1263-1275.

Aster, R., Borchers, B., Thurber, C., 2005. Parameter estimation and inverse problems, Academic Press, San Diego CA, 2005

Beck, A.E., 1977. Climatically perturbed temperature gradients and their effect on regional and continental heat-flow means, Tectonophysics, 41, 17-39.

Balling, N., Lind, G, Landström, O., Eriksson, K.G., Malmqvist, D., 1990. Thermal measurements from the deep Gravberg-1 well. R,D&D Report U(G) 1990/57, Swedish State Power Board, Vattenfall, 13 pp.

Birch, F., 1948. The effects of Pleistocene climatic variations upon geothermal gradients, Am. J. Sci., 246, 729-760.

Bredehoeft, J., 1967. Response of well-aquifer systems to earth tides. Journal of Geophysical Research, 72, 3075-3087.

Bredehoeft, J.D., Papadopoulos, I.S., 1965. Rates of vertical groundwater movements estimated from the Earth's thermal profile. Water Resour. Res., 1, 325-328.

Boulton, G.S., Caban, C.E., van Gijssel, K., 1995. Groundwater flow beneath ice sheets: Part I – Large scale patterns. Quaternary Science Reviews, 14, 545-562.

Boulton, G.S., Caban, P.E., van Gijssel, K., Leijnse, A., Punkari, M., van Weert, F.H.A., 1996. The impact of glaciation on the groundwater regime of Northwest Europe. Global and Planetary Change, 12, 397-413.

Boulton, G.S., Hagdorn, M., Maillot, P.B., Zatsepin, S., 2009. Drainage beneath ice sheets: groundwater-channel coupling, and the origin of esker systems from former ice sheets. Quaternary Science Reviews, 28, 621-638.

Čermak, V. 2009. Recurrence Quantification Analysis of Borehole Temperatures: Evidence of Fluid Convection. J. Bifurc. Chaos, 19(3), 889-902.

Čermak, V., Šafanda, J., Bodri, L., 2008a. Precise temperature monitoring in boreholes: evidence for oscillatory convection? Part 1: Experiments and field data. Int. J. Earth Sci. (Geol. Rundsch.), 97,365–373.

949 Čermak, V., Bodri, L., Šafanda, J., 2008b. Precise temperature monitoring in
950   boreholes: evidence for oscillatory convection? Part II: theory and
951   interpretation. Int. J. Earth Sci. (Geol Rundsch), 97, 375–384.
952 Čermak, V., Šafanda, J., Kresl, M., 2008c. Intra-hole fluid convection: High-
953   resolution temperature time monitoring. J. Hydrology, 348, 464-479.
954 Clauser, C., 1992. Permeability of crystalline rocks, Eos Trans. AGU, 73, p. 233 &
955   237.
956 Clauser, C. (Ed.), 2003. Numerical simulation of reactive flow in hot aquifers.
957   SHEMAT and Processing SHEMAT. Springer, Berlin, 332 pp.
958 Clauser, C., Giese, P., Huenges, E., Kohl, T., Lehmann, H., Rybach, L., Šafanda, J.,
959   Wilhelm, H., Windloff, K., Zoth, G., 1997. The thermal regime of the
960   crystalline continental crust: Implications from the KTB, J. Geophys. Res.,
961   102, 18417-18441.
962 Cutillo, P.A. and Bredhoeft, J.D., 2010. Estimating aquifer properties from the water
963   level response to Earth tides. Groundwater (DOI: 10.1111/j.1745-
964   6584.2010.00778.x).
965 Dahl-Jensen, D., Mosegaard, K., Gundestrip, N., Clow, G.D., Johnsen, S.J. , Hansen,
966   A.W., Balling, N., 1998. Past temperatures directly from the Greenland ice
967   sheet. Science, 282, 268-271.
968 Drury, M.J., 1984. Perturbations to temperature gradients by water flow in crystalline
969   formations. Tectonophysics, 102, 19-32.
970 Drury, M.J., Lewis, T.J., 1983. Water movement within Lac du Bonnet Batholith as
971   revealed by detailed thermal studies of three closely-spaced boreholes.
972   Tectonophysics, 95, 337-351.
973 Eppelbaum, L.V. and Kutasov, I.M., 2011. Estimation of the effect of thermal
974   convection and casing on the temperature regime of boreholes: a review. J.
975   Geophys. Eng., 8, R1-R10, doi:10.1088/1742-2132/8/1/R01.
976 Garcia, D., 2010. Robust smoothing of gridded data in one and higher dimensions
977   with missing values. Computational Statistics & Data Anal., 54, 1167–1178.
978 Glaznev, V. N., Kukkonen, I. T., Raevskii, A. B., Jokinen, J. , 2004. New data on
979   thermal flow in the central part of the Kola Peninsula, Doklady Earth Sci.,
980   396, 512–514.
981 Hales, A.L., 1937. Convection currents in geysers. Mon. Not. R. Astron. Soc.,
982   Geophys. Suppl., 4, 122–131.
983 Hänninen, P., Äikää, O., Sutinen R., Kukkonen, I., 2009. Borehole monitoring of
984   water table and temperature in bedrock and Quaternary sediments in
985   Outokumpu. In: Kukkonen, Ilmo T. (ed.), 2009. Outokumpu Deep Drilling
986   Project, Third International Workshop, Espoo, Finland, November 12-13,
987   2009, Programme and Abstracts. Geological Survey of Finland, Southern
988   Finland Office, Marine Geology and Geophysics, Report Q10.2/2009/61, 57-
989   60.
990 Heikkilä, M., Seppä, H., 2003. A 11,000 yr palaeotemperature reconstruction from the
991   southern boreal zone in Finland Quaternary Science Reviews, 22, 541-554
992 Heikkinen, P.J, Koivisto, E., Kukkonen, I.T., 2007. FIRE high resolution reflection
993   seismic survey in Outokumpu. In: Kukkonen, I.T. (Editor), 2007. Outokumpu
994   Deep Drilling Project, Second International Workshop, May 21-22, 2007, Espoo,
995   Finland. Programme and Extended Abstracts. Geological Survey of Finland,
996   Southern Finland Office, Marine Geology and Geophysics, Report
997   Q10.2/2007/29, 17-20.

998   Hsieh, P.A., Bredehoeft, J.D., Farr, J.M., 1987. Determination of aquifer
999   transmissivity from Earth tide analysis. Water Resources Res., 23, 1824-1832.
1000 Hubberten, H.W, Andreev, A., Astakhov, V.I., Demidov, I., Dowdeswell, J.A.,
1001   Henriksen, M., Hjort, C., Houmark-Nielsen, M., Jakobsson, M., Kuzmina, S.
1002   Larsen, E., Lunkka, J.P., Lys, A., Mangerud, J., Möller, P., Saarnisto, M.,
1003   Schirrmeister, L., Sher, A.V., Siegert, C., Siegert, M.J., Svendsen, J.I., 2004.
1004   The periglacial climate andenvironment in northern Eurasia during the Last
1005   Glaciation. Quat. Sci. Rev., 23, 1333–1357.
1006 Huhma, A., 1971. Geological map of Finland 1:100 000, Pre-Quaternary rocks, Sheet
1007   Sheet 4222 - Outokumpu, Geol. Surv. Finland, Espoo.
1008 Hurtig, E., Čermak, V., Haenel, R., Zui, V. (Editors), 1992. Geothermal Atlas of
1009   Europe. Hermann Haack, Gotha, 156 pp. + maps.
1010 Jansson, P., 2010. Ice sheet hydrology from observations. Swedish Nuclear Fuel and
1011   Waste Management Co., Technical Report TR-10-68, 59 pp.
1012 Jansson, P., Näslund, O. and Rodhe, L., 2007. Ice sheet hydrology – a review.
1013   Swedish Nuclear Fuel and Waste Management Co., Technical Report TR-06-
1014   34, 145 pp.
1015 Järvimäki, P., Puranen, M., 1979. Terrestrial heat flow in Finland. In: Terrestrial Heat
1016   Flow in Europe, edited by V. ermak and L. Rybach, Springer, Berlin, 172-
1017   178.
1018 Jessop, A.M., 1971. The distribution of glacial perturbation of heat flow in Canada,
1019   Can. J. Earth Sci., 8, 162-166.
1020 Koistinen, T., Stephens, M. B., Bogatchev, V., Nordgulen, Ø. Wennerström, M.,
1021   Korhonen, J., 2001, Geological map of the Fennoscandian Shield, scale 1:2
1022   000 000: Geol. Surv. Finland, Norway and Sweden and the North-West Dept.
1023   of Nat. Res. of Russia.
1024 Kremenetsky, A.A., Ovchinnikov, L.N., 1986. The Precambrian continental crust: Its
1025   structure, composition and evolution as revealed by deep drilling in the USSR,
1026   Precambr. Res., 33, 11-43.
1027 Kukkonen, I.T., 1987. Vertical variation of apparent and palaeoclimatically corrected
1028   heat flow densities in the central Baltic Shield, J. Geodyn. 8, 33-53.
1029 Kukkonen, I.T., 1988. Terrestrial heat flow and groundwater circulation in the
1030   bedrock in the central Baltic Shield, Tectonophysics, 156, 59-74.
1031 Kukkonen, I. T., 1995. Thermal aspects of groundwater circulation in bedrock and its
1032   effect on crustal geothermal modelling in Finland, the central Fennoscandian
1033   Shield. In: N. Balling and E.R. Decker (Editors), Heat Flow and Thermal
1034   Regimes of Continental Lithosphere, Tectonophysics, 244, 119-136.
1035 Kukkonen, I.T. (ed.), 2009. Outokumpu Deep Drilling Project, Third International
1036   Workshop, Espoo, Finland, November 12-13, 2009, Programme and
1037   Abstracts. Geological Survey of Finland, Southern Finland Office, Marine
1038   Geology and Geophysics, Report Q10.2/2009/61, 92 pp.
1039 Kukkonen, I.T. (ed.), 2011. Outokumpu Deep Drilling Project 2003-2010. Geological
1040   Survey of Finland, Special Paper, 51, 252 pp.
1041 Kukkonen, I. T., Clauser, C., 1994. Simulation of heat transfer at the Kola deep-hole
1042   site: implication for advection, heat refraction and paleoclimatic effects.
1043   Geophys. J. Int., 116, 409–420.
1044 Kukkonen, I. T., Jõeleht, A., 2003. Weichselian temperatures from geothermal heat
1045   flow data, J. Geophys. Res., 108(B3), 2163, doi:10.1029/2001JB001579.

1046 Kukkonen, I., Lindberg, A. 1998. Thermal properties of rocks at the investigation
1047   sites: measured and calculated thermal conductivity, specific heat capacity and
1048   thermal diffusivity. Posiva Oy, Work. Rep., 98-09e, 29 pp.
1049 Kukkonen, I.T., Šafanda, J., 1996. Palaeoclimate and structure: the most important
1050   factors controlling subsurface temperatures in crystalline rocks. A case history
1051   from Outokumpu, eastern Finland. Geophys. J. Int., 126, 101-112.
1052 Kukkonen, I.T., Golovanova, I.V., Khachay, Yu.V., Druzhinin, V.S., Kosarev, A.M.,
1053   Schapov, V.A., 1997. Low geothermal heat flow of the Urals fold belt -
1054   implication of low heat production, fluid circulation or palaeoclimate?
1055   Tectonophysics, 276, 63-85.
1056 Kukkonen, I. T., Gosnold, W. D., Šafanda, J., 1998. Anomalously low heat flow
1057   density in eastern Karelia, Baltic shield: a possible palaeoclimatic signature,
1058   Tectonophysics, 291(1-4), 235–249.
1059 Kukkonen, I.T., Heikkinen, P., Ekdahl, E., Hjelt, S.-E., Yliniemi, J., Jalkanen, E.,
1060   FIRE Working Group, 2006. Acquisition and geophysical characteristics of
1061   reflection seismic data on FIRE transects, Fennoscandian Shield. In:
1062   Kukkonen, I.T. and Lahtinen, R. (editors), Finnish Reflection Experiment
1063   2001-2005. Geological Survey of Finland, Special Paper 43, pp. 13-43 +11
1064   appendices.
1065 Lemieux, J.-M., Sudicky, E.A., 2010. Simulation of groundwater age evolution during
1066   the Wisconsinian glaciation over the Canadian landscape. Environ. Fluid
1067   Mech., 10, 91-102.
1068 Lemieux, J.-M., Sudicky, E.A., Peltier, W.R., Tarasov, L., 2008. Dynamics of
1069   groundwater recharge and seepage over the Canadian landscape during the
1070   Wisconsinian glaciation. Journal of Geophysical Research, 113, F01011,
1071   doi:10.1029/2007/JF000838, 18 pp.
1072 Lunkka, J.P., Saarnisto, M., Gey, V., Demidov, I., Kiselova, V., 2001. Extent and age
1073   of the Last Glacial Maximum in the southeastern sector of the Scandinavian
1074   Ice Sheet. Gl. Planet. Change, 31, 407– 425.
1075 Luterbacher, J., Dietrich, D., Xoplaki, E., Grosjean, M., Wanner, H., 2004. European
1076   seasonal and annual temperature variability, trends and extremes since 1500.
1077   Science, 303, 1499-1503 (with supporting online material).
1078 Majorowicz, J., Šafanda, J., 2007. Heat flow variation with depth in Poland: evidence
1079   from equilibrium temperature logs in 2.9-km-deep well Torun-1. Int. J. Earth
1080   Sci. (Geol. Rundsch.), DOI 10.1007/s00531-007-0210-2.
1081 Majorowicz, J., Wybraniec, S., 2010. New terrestrial heat flow map of Europe after
1082   regional paleoclimatic correction application. Int. J. Earth Sci.,
1083   doi:10.1007/s00531-010-0526-1, published online.
1084 Manning, C., Ingebritsen, S.E., 1999. Permeability of the continental crust:
1085   Implications from geothermal data and metamorphic systems. Rev. Geophys.,
1086   37, 127–150
1087 Mareschal, J.-C., Rolandone, F., Bienfait, G., 1999. Heat flow variations in a deep
1088   borehole near Sept-Iles, Québec, Canada: Palaeoclimatic interpretation and
1089   implications for regional heat flow estimates. Geophys. Res. Lett., 26, 2049-
1090   2052.
1091 Mottaghy, D., Popov, Y. A., Schellschmidt, R., Clauser, C., Kukkonen, I. T., Nover,
1092   G., Milanovsky, S., Romushkevich, R. A., 2005. New heat flow data from the
1093   immediate vicinity of the Kola superdeep borehole: Vertical variation in heat
1094   flow density confirmed and attributed to advection, Tectonophysics, 401(1–2),
1095   119–142.

1096 Munk, W.H. and MacDonald, G.J.F., 1960. The rotation of the Earth: A geophysical
1097   discussion. Cambridge Univ. Press, London, 323 pp.
1098 Newman, G. A., Hoversten, G. M., 2000. Solution strategies for two- and three-
1099   dimensional electromagnetic inverse problems. Inverse Problems, 16, 1357-
1100   1375.
1101 Nolet, G., Montelli, R., Virieux, J. (1999). Explicit, approximate expressions for the
1102   resolution and a-posteriori covariance of massive tomographic systems.
1103   Geophys. J. Int., 138, 36-44.
1104 Papunen, H., Gorbunov, G.I. (eds), 1985. Nickel deposits of the Baltic Shield and
1105   Scandinavian Caledonides. Geol. Surv. Finland, Bull. 333.
1106 Paterson, W.S.B., 1994. The physics of glaciers, 3rd ed., Elsevier, Oxford, 480 pp.
1107 Peltonen, P., Kontinen, A., Huhma, H., Kuronen, U., 2008. Outokumpu revisited:
1108   New mineral deposit model for the mantle peridotite-associated Cu–Co–Zn–
1109   Ni–Ag–Au sulphide deposits. Ore Geol. Rev., 33, 559–617.
1110 Person, M., McIntosh, J., Bense, V. and Remenda, V.H., 2007. Pleistocene hydrology
1111   of North America: the role of ice sheets in reorganizing groundwater flow
1112   systems. Reviews of Geophysics, 45, RG3007, 28 pp.,
1113   doi:10.1029/2006RG000206.
1114 Popov, Yu. A., Pimenov, V.P. Pevzner, L.A. Romushkevich, R.A., Popov, E. Yu.,
1115   1998a. Geothermal characteristics of the Vorotilovo deep borehole drilled into
1116   the Puchezh-Katunk impact structure, Tectonophysics, 291, 205-223.
1117 Popov, Yu. A., Romushkevich, R.A., Popov, E.Yu., Bashta, K.G., 1999b.
1118   Geothermicheskiy characteristikiy razreza SG-4 (in Russian) (Geothermal
1119   characteristics of profile SG-4). In: B.N. Khakhaev, A.F. Morozov, V.I.
1120   Gorbachev, L.A. Pevzner, K.G. Bashta, A. J. Dokuchaev, V.V. Kenig, N.V.
1121   Mezelovskyi and M.S. Rapoport (editors), Resultatiy Bureniya i Issledovannih
1122   Uralskoy Sverghlubukoy Shkvashiny (SG-4) (Results of drilling and
1123   investigations of the Ural super-deep borehole (SG-4)), Ministerstvo
1124   Prirodnyih RF, Jaroslavl, 77-88.
1125 Popov, Y. A., Pevzner, S. L., Pimenov, V. P., Romushkevich, R. A., 1999. New
1126   geothermal data from the Kola superdeep well SG-3. Tectonophysics, 306,
1127   345–366.
1128 Ramey, H.J., 1962. Well-bore heat transmission. J. Pet. Technol., 14, 427-435.
1129 Rath, V., Mottaghy, D., 2007. Smooth inversion for ground surface temperature
1130   histories: estimating the optimum regularization parameter by generalized
1131   cross-validation. Geophys. J. Int., 171, 1440–1448.
1132 Rybach, L., 1973. Warmeproduktionsbestimmungen an Gesteinen der Schweizer
1133   Alpen. Beitr. Geol. Schweiz, Geotech. Ser. 51, 43 pp.
1134 Šafanda, J., Szewzyk, J., Majorowicz, J. A., 2004. Geothermal evidence of very low
1135   glacial temperatures on a rim of the Fennoscandian ice sheet, Geophys. Res.
1136   Letters, 31, L07211, doi:10.1029/2004GL019547.
1137 Säntti, J., Kontinen, A., Sorjonen-Ward, P., Johanson, B., Pakkanen, L., 2006.
1138   Metamorphism and chromite in serpentinized and carbonate-silica–altered
1139   peridotites of the Paleoproterozoic Outokumpu-Jormua ophiolite belt, eastern
1140   Finland. Int. Geol. Rev., 48, 494–546.
1141 Seppä, H., Poska, A., 2004. Holocene annual mean temperature changes in Estonia
1142   and their relationship to solar insolation and atmospheric circulation patterns
1143   Quat. Res., 61, 22-31
1144 Slagstad, T., Balling, N., Elvebakk, H., Midttømme, K., Olesen, O., Olsen, L., Pascal,
1145   C., 2009. Heat-flow measurements in Late Palaeoproterozoic to Permian

1146   geological provinces in south and central Norway and a new heat-flow map of
1147   Fennoscandia and the Norwegian-Greenland Sea. Tectonophysics, 473, 341-
1148   361.
1149 Sokolnicki, M., Heikkinen, P., 2008. Difference Flow Measurements in Outokumpu
1150   Deep Hole OKUR2500. Posiva Oy, Finland, Work. Rep., 2008-87, 19 pp.
1151 Spane, F.A., 2002. Considering barometric pressure in groundwater flow
1152   investigations. Water Resources Res., 38, no. 6, doi 10.1029/2001WR000701.
1153 Svendsen, J.I., Astakhov, V.I., Bolshianov, D.Yu., Demidov, I., Dowdeswell, J.A.,
1154   Gataullin, V., Hjort, C., Hubberten, H.W., Larsen, E., Mangerud, J., Melles,
1155   M., Möller, P., Saarnisto, M., Siegert, M.J., 1999. Maximum extent of the
1156   Eurasian ice sheets in the Barents and Kara Sea region during the
1157   Weichselian. Boreas, 28, 234-242.
1158 Svendsen, J.I, Alexanderson, H., Astakhov, V.I., Demidov, I., Dowdeswell, J.A.,
1159   Funder, S., Gataullin, V., Henriksen, M., Hjort, C., Houmark-Nielsen, M.,
1160   Hubberten, H.W., Ing! olfsson, O., Jakobsson, M., Kjær, K.H., Larsen, E.,
1161   Lokrantz, H., Lunkka, J.-P., Lys, A., Mangerud, J., Matioushkov, A., Murray,
1162   A., Möller, P., Niessen, F., Nikolskaya, O., Polyak, L., Saarnisto, M., Siegert,
1163   C., Siegert, M.J., Spielhagen, R.F., Stein, R., 2004. Late Quaternary ice sheet
1164   history of northern Eurasia. Quat. Sci. Rev., 23, 1229-1271.
1165 Tarvainen, A.-M., 2006. Identification of water-bearing structures in the Outokumpu
1166   Deep Drill hole by geophysical well logging. Master's thesis (technology),
1167   Helsinki University of Technology, Department of Civil and Environmental
1168   Engineering, 93 p. (in Finnish with English abstract).
1169 Ukkonen, P., Lunkka, J.P., Jungner, H., Donner, J., 1999. New radiocarbon dates
1170   from Finnish mammoths indicating large ice free areas in Fennoscandia during
1171   the Middle Weichselian. J. Quat. Sci., 14/7, 711– 714.
1172 Vaikmäe, R., Vallner, L., Loosli, H.H., Blaser, E.C. and Juillard-Tardent, M., 2005.
1173   Palaeogroundwater of glacial origin in the Cambrian-Vendian aquifer of
1174   northern Estonia. Geological Society, London, Special Publications, 189, 17-
1175   27.
1176 Västi, K., 2005. Outokumpu deep drill core: geological report. Geological Survey of
1177   Finland, Report M 52.5/4222/04/R2500, 24.03.2006, 13 pp.
1178 Wahba, G., 1990. Spline Models for Observational Data. Society for Industrial
1179   Mathematics, Philadelphia.
1180 Van der Kamp, G., Bachu, S., 1989. Use of dimensional analysis in the study of
1181   thermal effects of various hydrogeological regimes. In: A.E. Beck, G. Garven
1182   and L. Stegena (Editors), Hydrogeological Regimes and Their Subsurface
1183   Thermal Effects. Am. Geophys. Union Geophys. Monogr.,47, 23-28.

1184
1185
1186   **Figure 1.** Location of the Outokumpu Deep Drill Hole site on a simplified geological
1187   map of the Outokumpu area in eastern Finland. Inset shows the location of
1188   Outokumpu in the Fennoscandian Shield. A: Archaean (>2.5 Ga); SK: Svecokarelian
1189   (2.5-1.75 Ga); PS: Post-Svecokarelian (1.7-1.2 Ga); SN: Sveconorwegian (1.8-0.9
1190   Ga); EEP: East European Platform. Adapted from from Huhma (1971), Papunen and
1191   Gorbunov (1985), Koistinen et al. (2001) and Peltonen et al. (2008).
1192
1193   **Figure 2.** The main lithological units of the Outokumpu Deep Drill Hole.
1194
1195   **Figure 3.** 3D-presentation of high-resolution seismic lines in Outokumpu. The model
1196   represents migrated data by the FIRE project (Kukkonen et al., 2006; Heikkinen et al.,
1197   2007) and a lithological surface map. The seismic sections extend to 5 km depth. The
1198   amplitude scale of the reflectors has been color-coded for indicating higher reflection
1199   amplitudes. Layers of strong reflectivity (lilac tones) are associated to the ophiolite-
1200   derived rocks types and poorly reflective areas to mica schist and pegmatitic granite.
1201   The 2D forward geothermal model (Fig. 8) was constructed using the OKU1 seismic
1202   section and the crustal scale FIRE3 profile running on the same transect. Seismic data
1203   processing: P. Heikkinen, Institute of Seismology, University of Helsinki.
1204
1205   **Figure 4.** Temperature logs obtained during drilling breaks and immediately after
1206   drilling. For dates of the logs and shut-in times, see Table 1. The logs 'OKU-290'
1207   (logged in 1963; Järvimäki and Puranen, 1979) and 'OKU-741' (logged in 1985;
1208   Kukkonen, 1988), are from other shallower holes of the Outokumpu area showing
1209   typical (undisturbed) formation temperatures in the uppermost 1 km.
1210
1211   **Figure 5.** Temperature and fluid electrical conductivity logs in the Outokumpu deep
1212   drill hole in 2005-2008. Arrows pointing to the left indicate depths of saline formation
1213   fluid flowing into the hole, and arrows to the right out from the hole, respectively. Up
1214   and down pointing arrows indicate the flow in the hole. 'Fractures' column indicates
1215   interpreted fractures from sonic, galvanic and calliper logs (adapted from Tarvainen,
1216   2006). 'Lithology' shows the rock types (blue: metasediments; green and orange:
1217   ophiolite-derived serpentinite and skarn rocks; pink: pegmatitic granite).

1218

1219

1220   **Figure 6.** Outokumpu deep drill hole geothermal results. From left: lithological

1221   column (according to Västi, 2005; blue: metasediments; green and orange: ophiolite-

1222   derived serpentinite and skarn rocks; pink: pegmatitic granite), reduced temperature

1223   (log of Sept '08, reduction gradient 13 mKm^{-1}), electrical conductivity of drill hole

1224   water with the hydraulically conductive fractures estimated from density, acoustic and

1225   galvanic logs ('Fractures', adapted from Tarvainen, 2006) , radiogenic heat

1226   production rate calculated from density and gamma ray U-Th-K logs, thermal

1227   conductivity measured in the lab, moving average of thermal conductivity (20 m

1228   window), moving average of temperature gradient (20 m window) and calculated heat

1229   flow density (green line: heat flow from moving averages of conductivity and

1230   gradient; red line: average heat flow calculated at 100 m intervals). See also Table 2.

1231

1232   **Figure 7.** Temperature recorded by a stationary temperature probe located at 1390 m.

1233   Sampling interval 5 sec. Note the detailed oscillatory character of the temperature

1234   time variations in both inserted figures demonstrating the enlarged "1-hour" and/or

1235   "ten-minutes" time intervals. Slightly decreasing temperature corresponds to the

1236   unsettled probe temperature equilibration.

1237

1238   **Figure 8.** 2D model of the Outokumpu structure used in forward conductive heat

1239   transfer modelling. The applied thermal parameter values are listed in Table 3.

1240

1241   **Figure 9.** Ground surface temperature variation used as the upper boundary condition

1242   in the 2D transient modelling.

1243

1244   **Figure 10.** Results of the 2D forward transient conduction model at the location of the

1245   Outokumpu deep hole. Dotted lines represent the measured temperatures (05-SEP-

1246   2008) and solid lines temperatures simulated with the model (Figs. 8 and 9). The right

1247   panel shows the temperatures reduced with a constant gradient of 13 mKm^{-1}.

1248

1249   **Figure 11.** Simulated steady-state (*Top*) and present (*Bottom*) values of vertical heat

1250   flow density (in units of mWm^{-2}) of the 2D forward transient modelling. The applied

1251   surface temperature is shown in Fig. 9 and modelled rock type domains in Fig. 8, and

1252   thermal parameters in Table 3.

1253

1254   **Figure 12.** Results of the upscaling of measured temperatures (upper panels) and

1255   thermal conductivities (lower panels) to the numerical grid. Elementary descriptive

1256   statistics lead to a very small average of -0.0002 K for temperature, and standard

1257   deviations for the residuals of 0.007 K. The situation is worse with thermal

1258   conductivity, where the upscaling process leads to considerable smoothing. For the

1259   harmonic mean upscaling the corresponding values are 0.10235 $Wm^{-1}K^{-1}$ and 0.65983

1260 $Wm^{-1}K^{-1}$, respectively.

1261

1262   **Figure 13.** *Top:* Results of smooth inversion for different values of basal heat flow

1263   values assumed at a depth of 5000 m. The model assumes a 1D layered structure with

1264   conductivity and heat production in the uppermost 2.5 km as determined from logs

1265   and laboratory measurements in the deep hole. Between at 2.5 – 5 km, a constant

1266   conductivity of 2.9 $Wm^{-1}K^{-1}$ and heat production were assumed. The latter was set to

1267   the value of the pegmatitic granite reduced by a factor of 0.8. *Center*: Basal heat flow

1268   is kept constant but the heat production of pegmatitic granite is varied at 1 $\mu W\ m^{-3}$

1269   steps. Assuming that heat production 3 $\mu W\ m^{-3}$ is representative (cf. Table 3 and Fig.

1270   6), we may conclude that the true value of basal heat flow is $32 – 34\ mW\ m^{-2}$.

1271   *Bottom:* "Optimum" GSTH with a basal HFD of 32 $mW\ m^{-2}$ and heat production of 3

1272 $\mu W\ m^{-3}$ (solid line). Also shown are 2σ error bars (dashed), and the paleotemperature

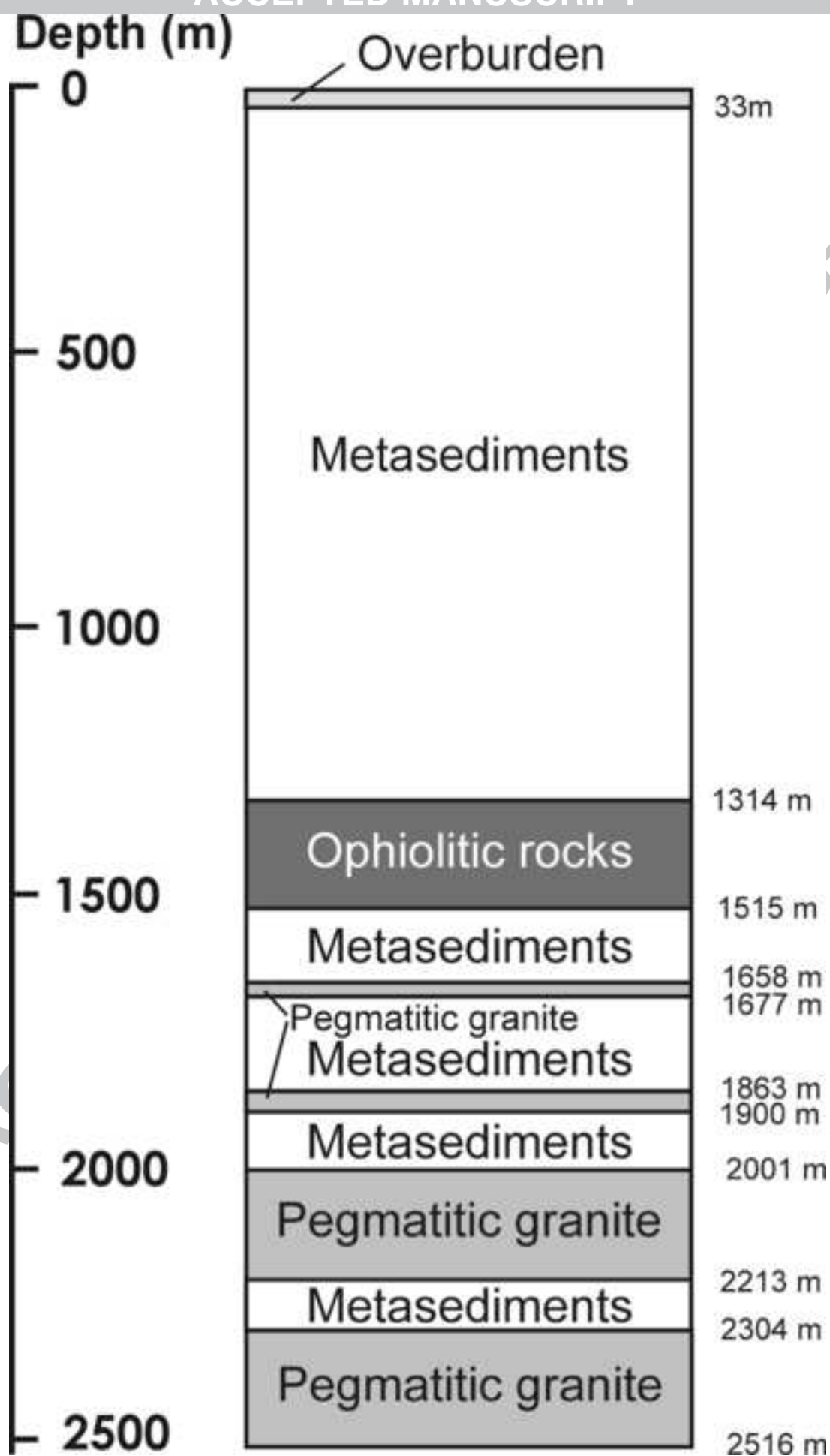1273   reconstructions of Luterbacher et al. (2004), and Heikkilä & Seppä (2003).

1274

1275   **Figure 14.** Top: Root-mean-square values of inversion results for combinations of

1276   basal HFD and pegmatite heat production. The results indicate a valley of best fit

1277   clearly visible in the contours of RMS. All have a RMS value just below 0.9. *Bottom*:

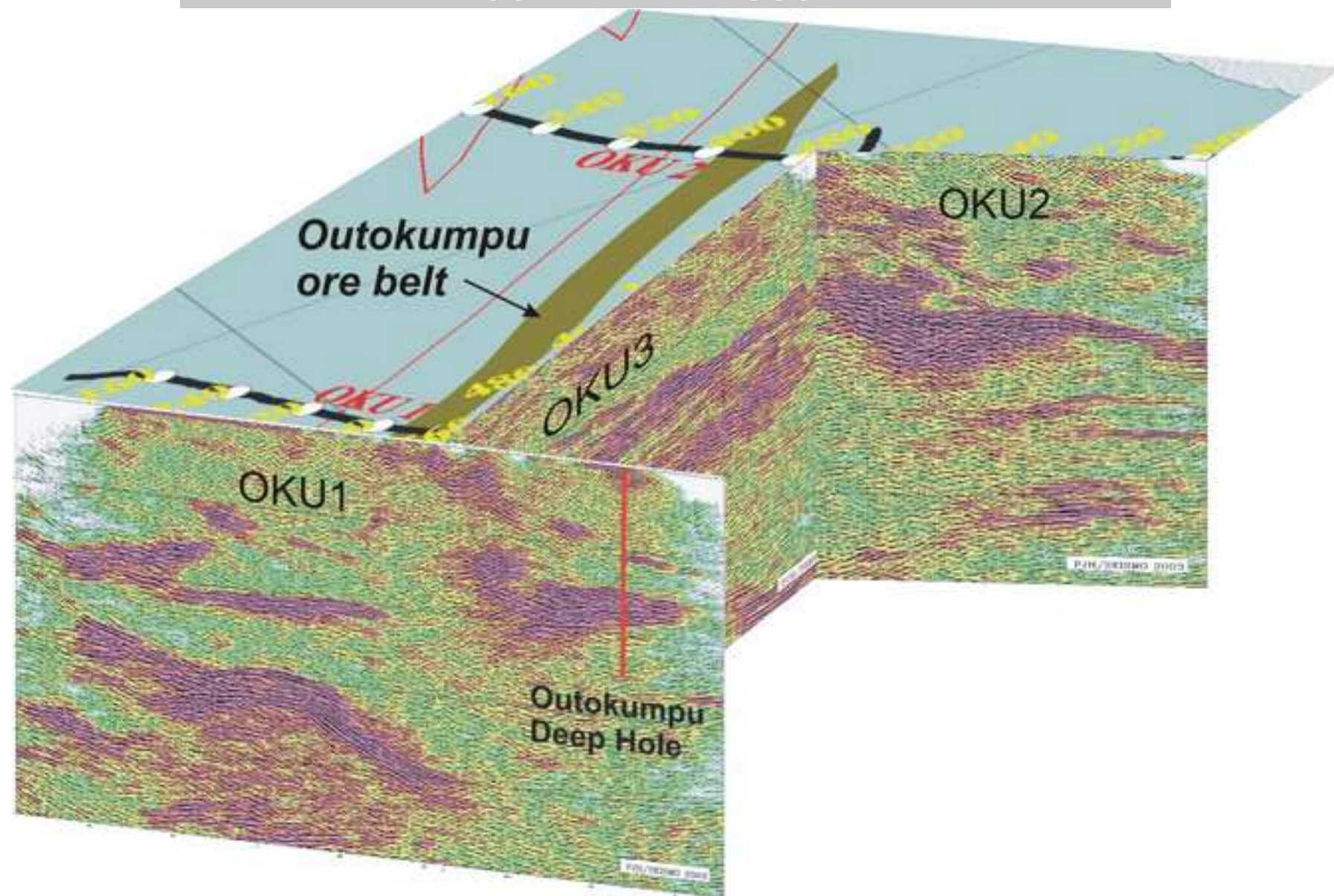1278   LGM temperatures of these best fit models seem to be well constrained near -4 ºC.

1279

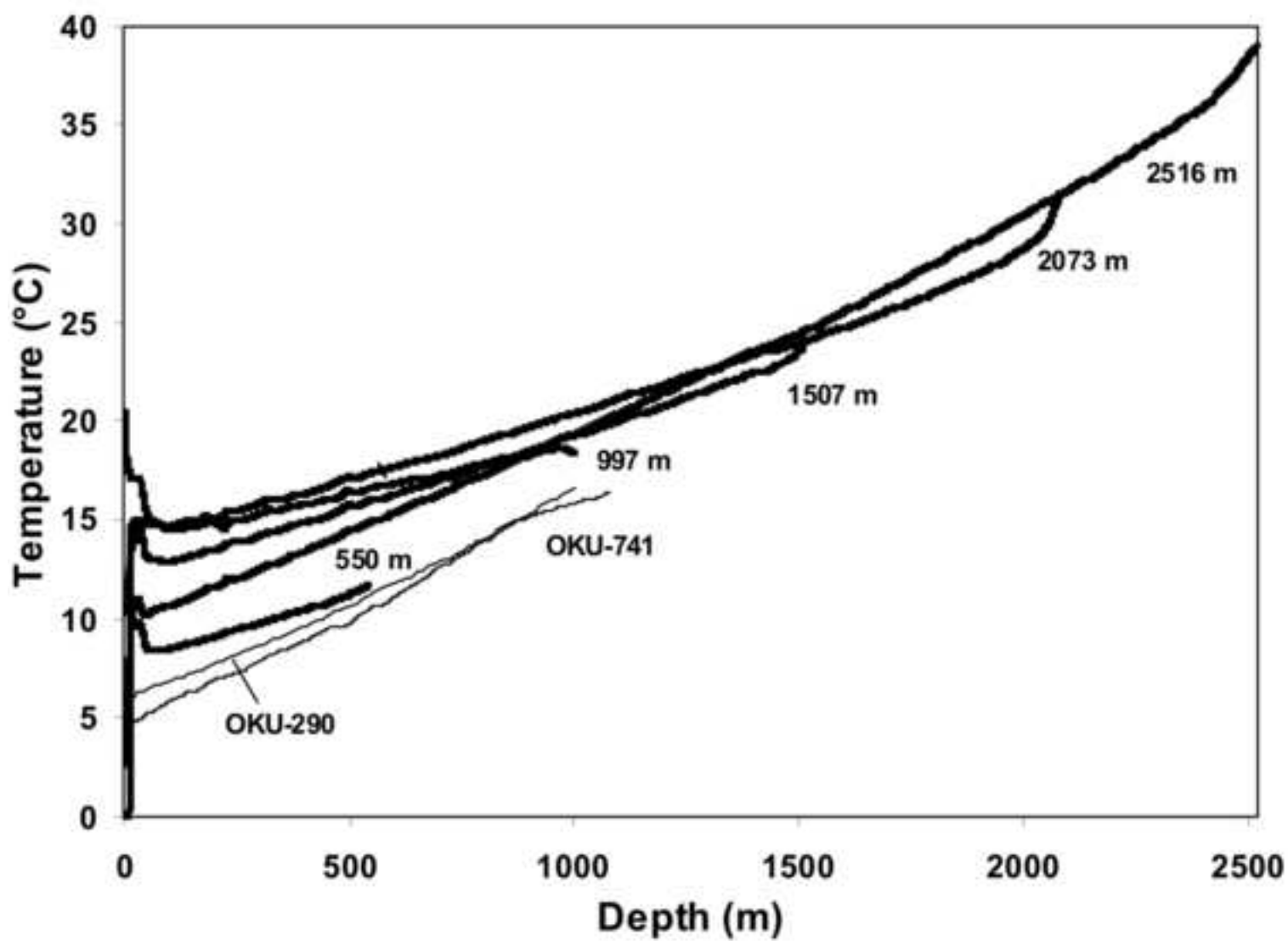Ophiolite rocks 1.95-1.97 Ga
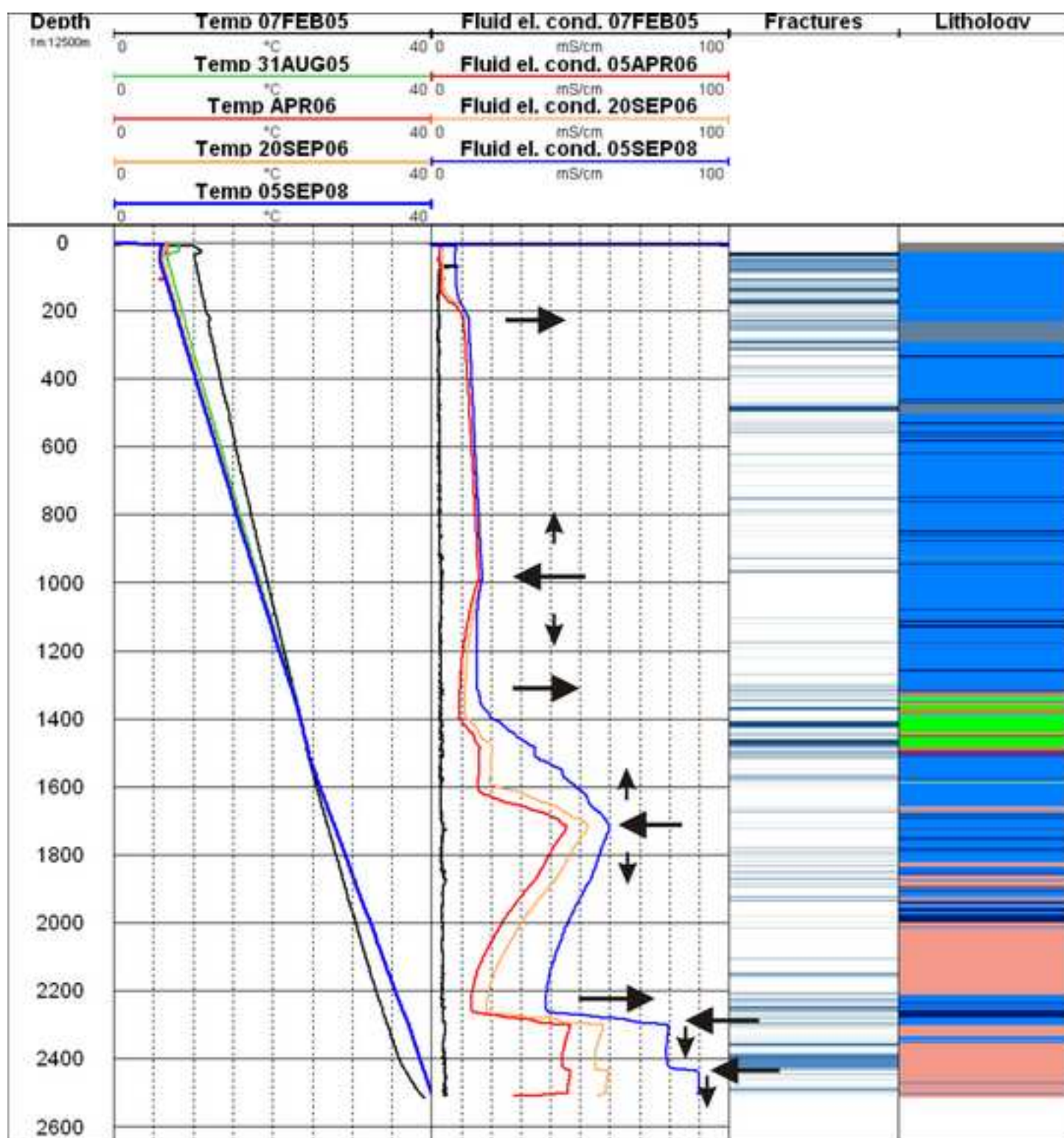(Outokumpu rock type assemblage)

Granitoids 1.80-1.89 Ga

Autochthonous metaturbidites
(Lower Kaleva)

Allochthonous metaturbidites
(Upper Kaleva)

Quartzite + minor metavolcanics
& calc-silicate rocks (Jatulian)

A Archaean

Figure(s)

Fig. 3

Fig. 4

Fig. 5

Fig. 6

OUTOKUMPU

(a) one hour interval

(b) six minutes interval

TEMPERATURE, °C

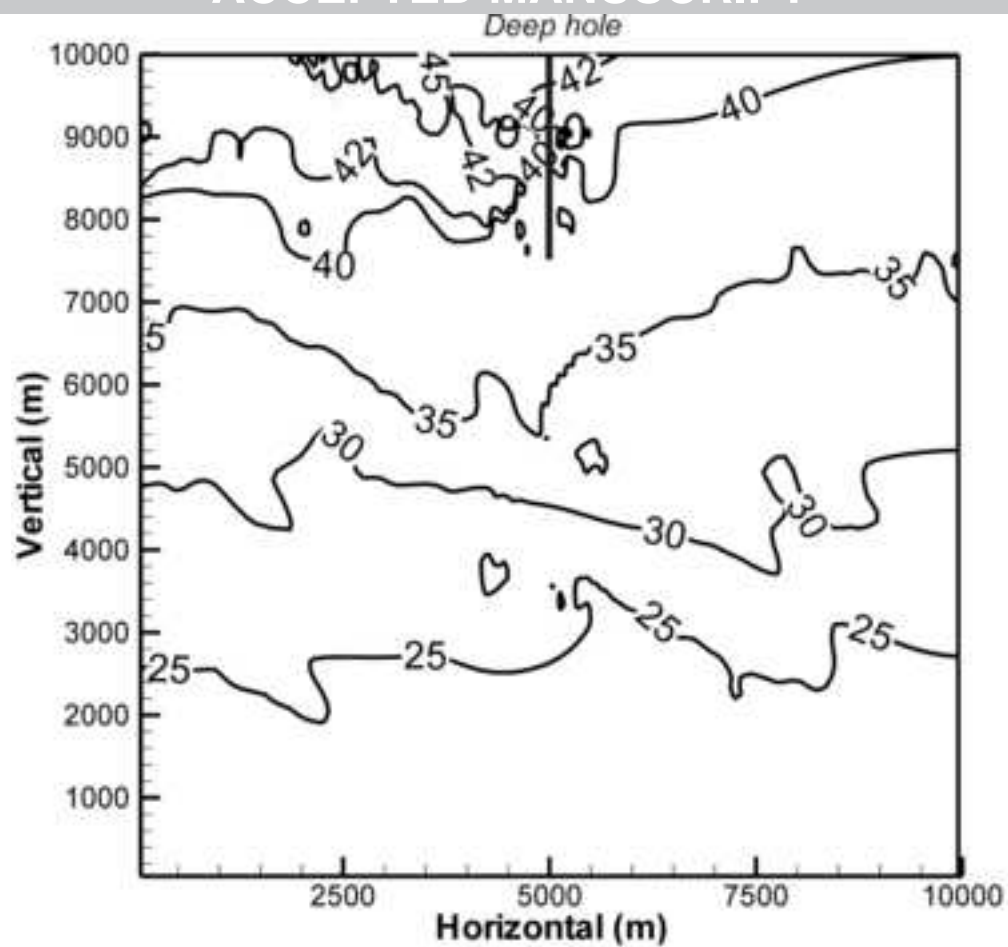TIME, hours since Aug 31, 2005, 0:00
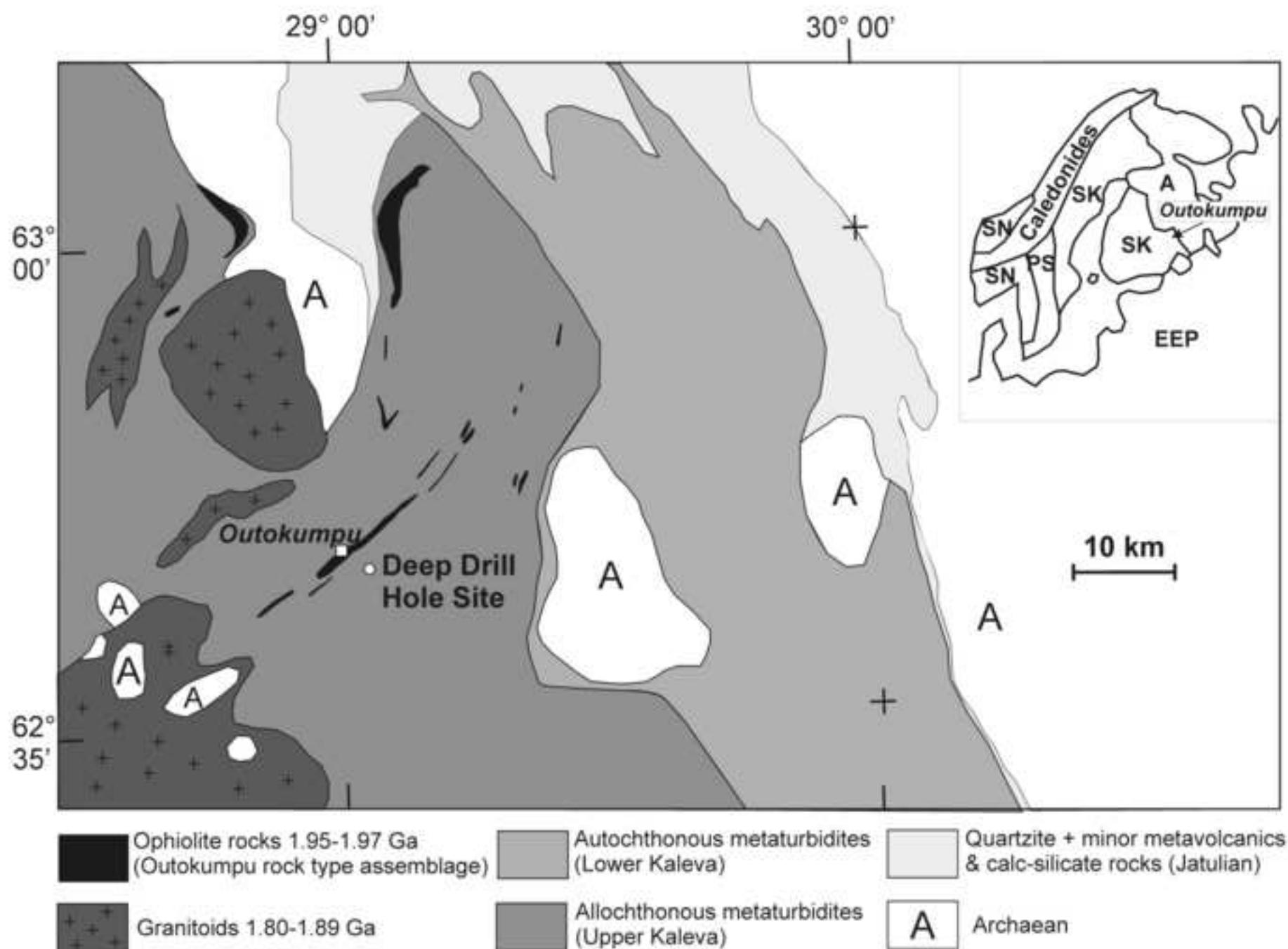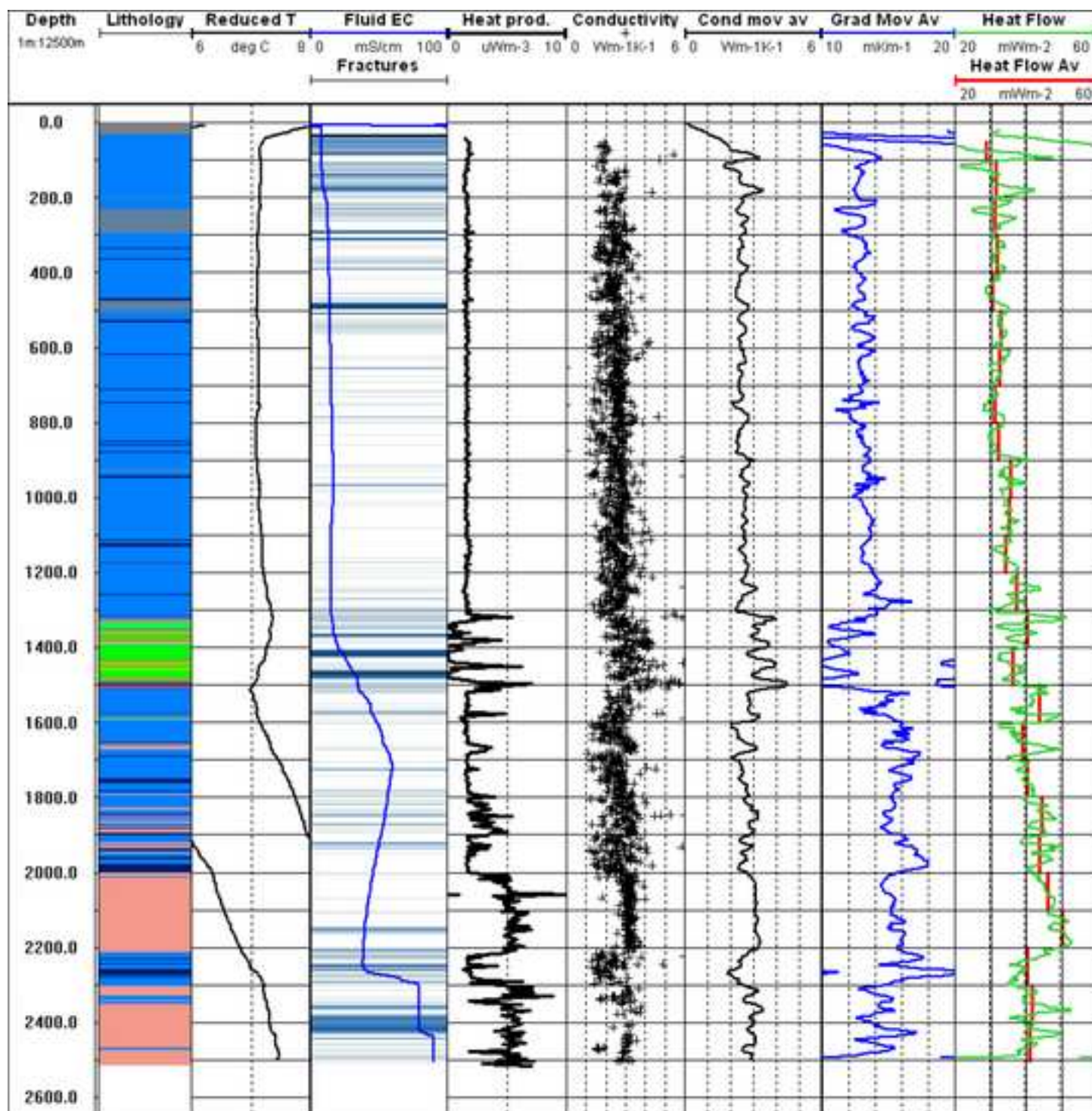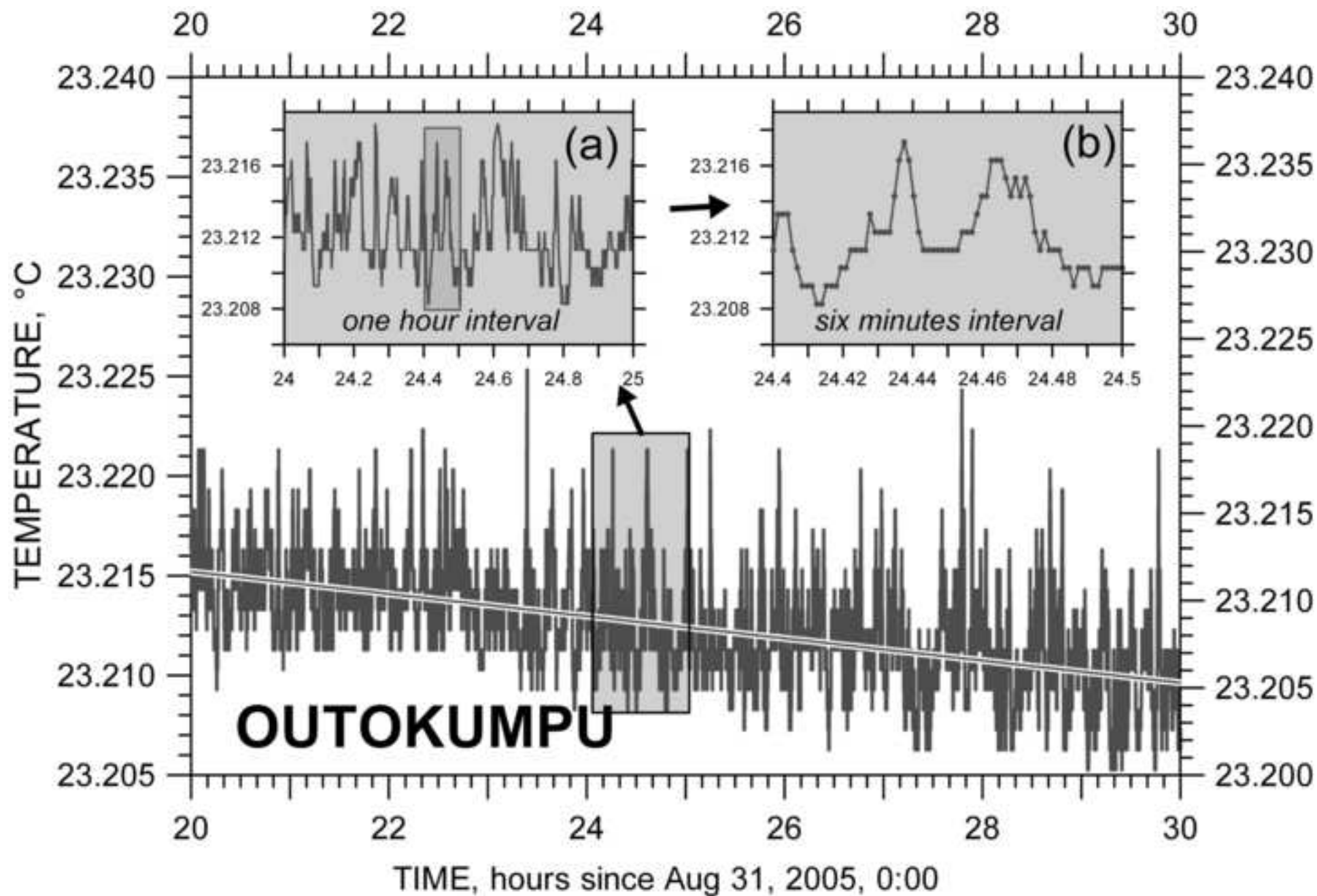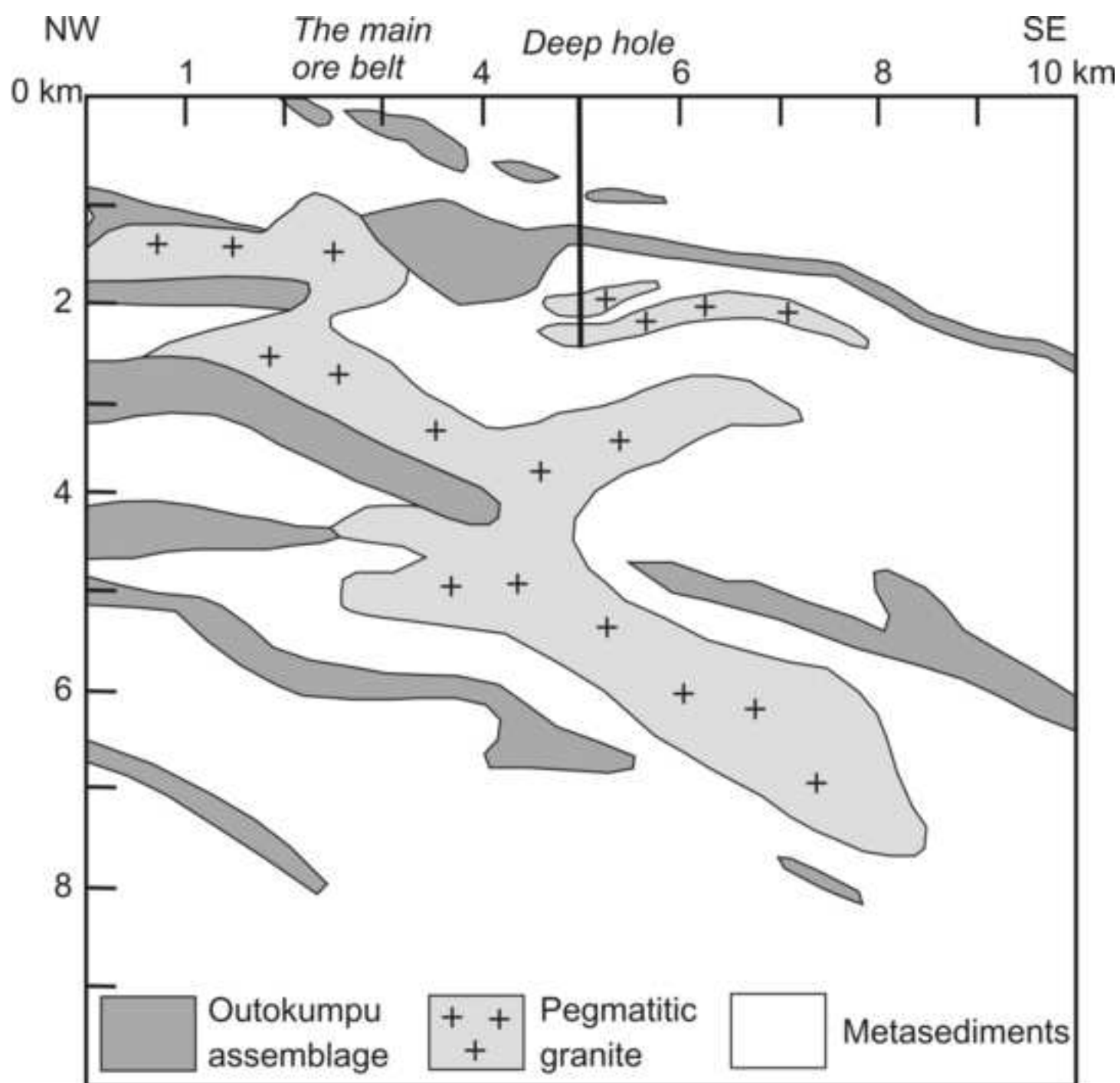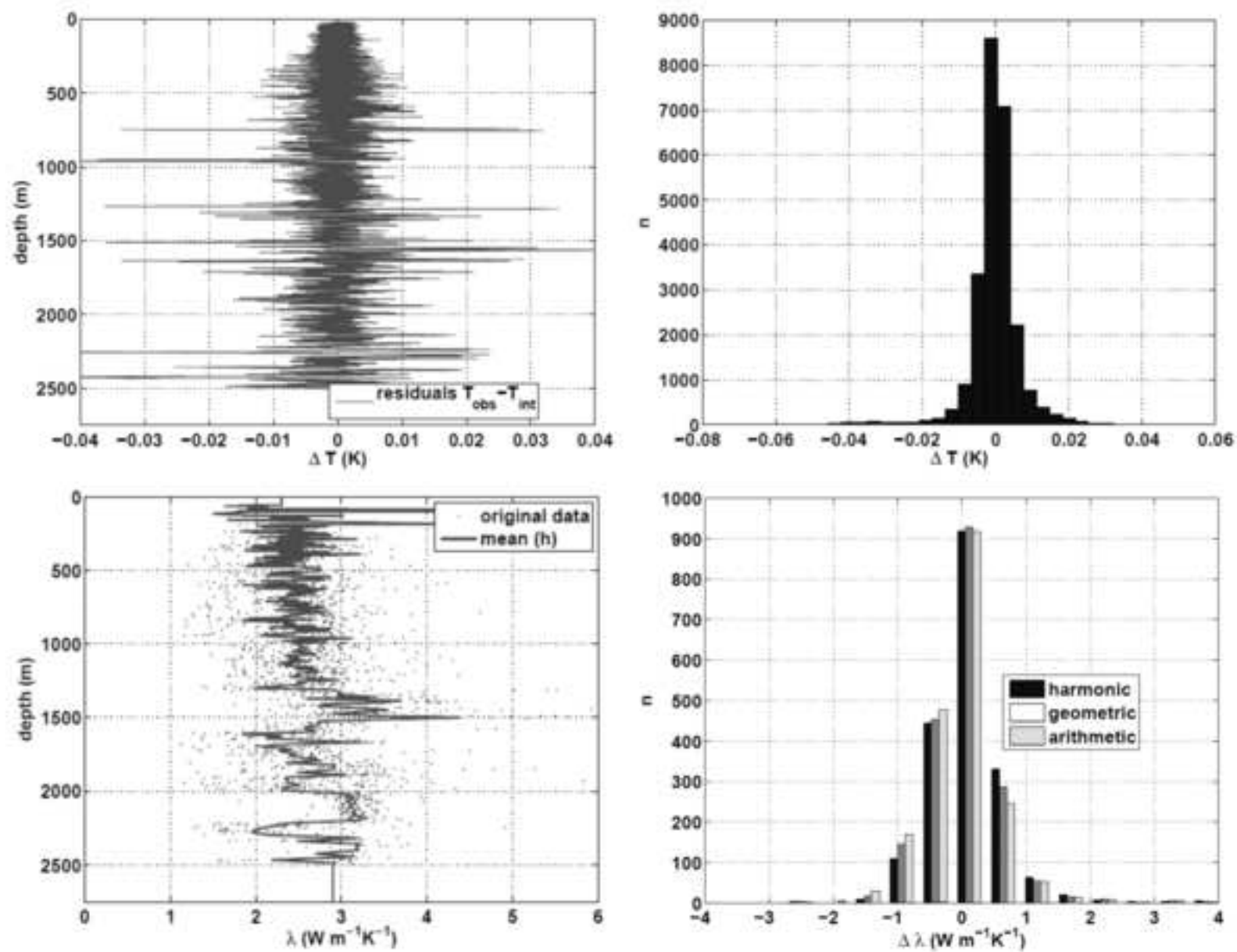
Fig. 8
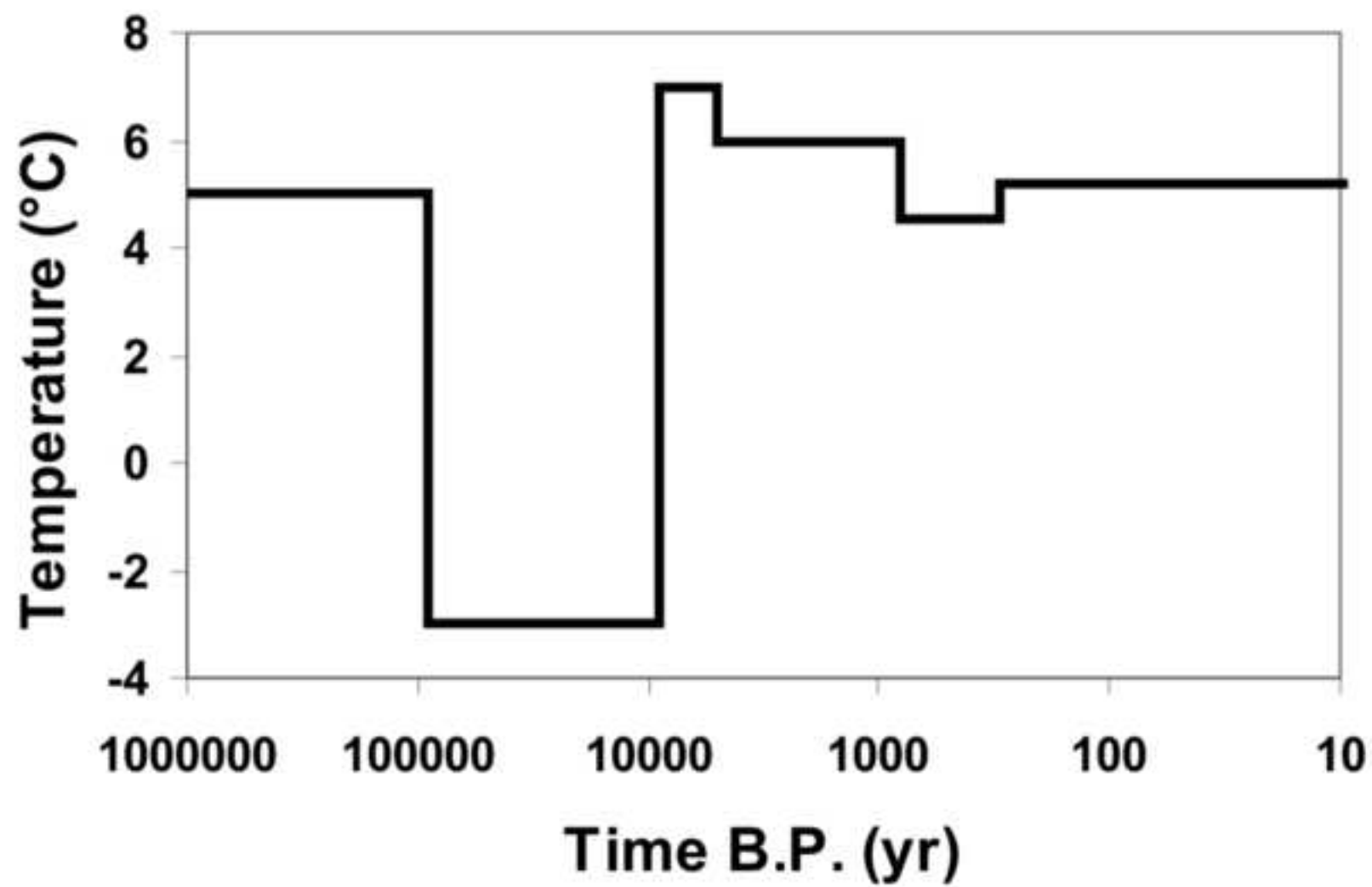
Fig. 9
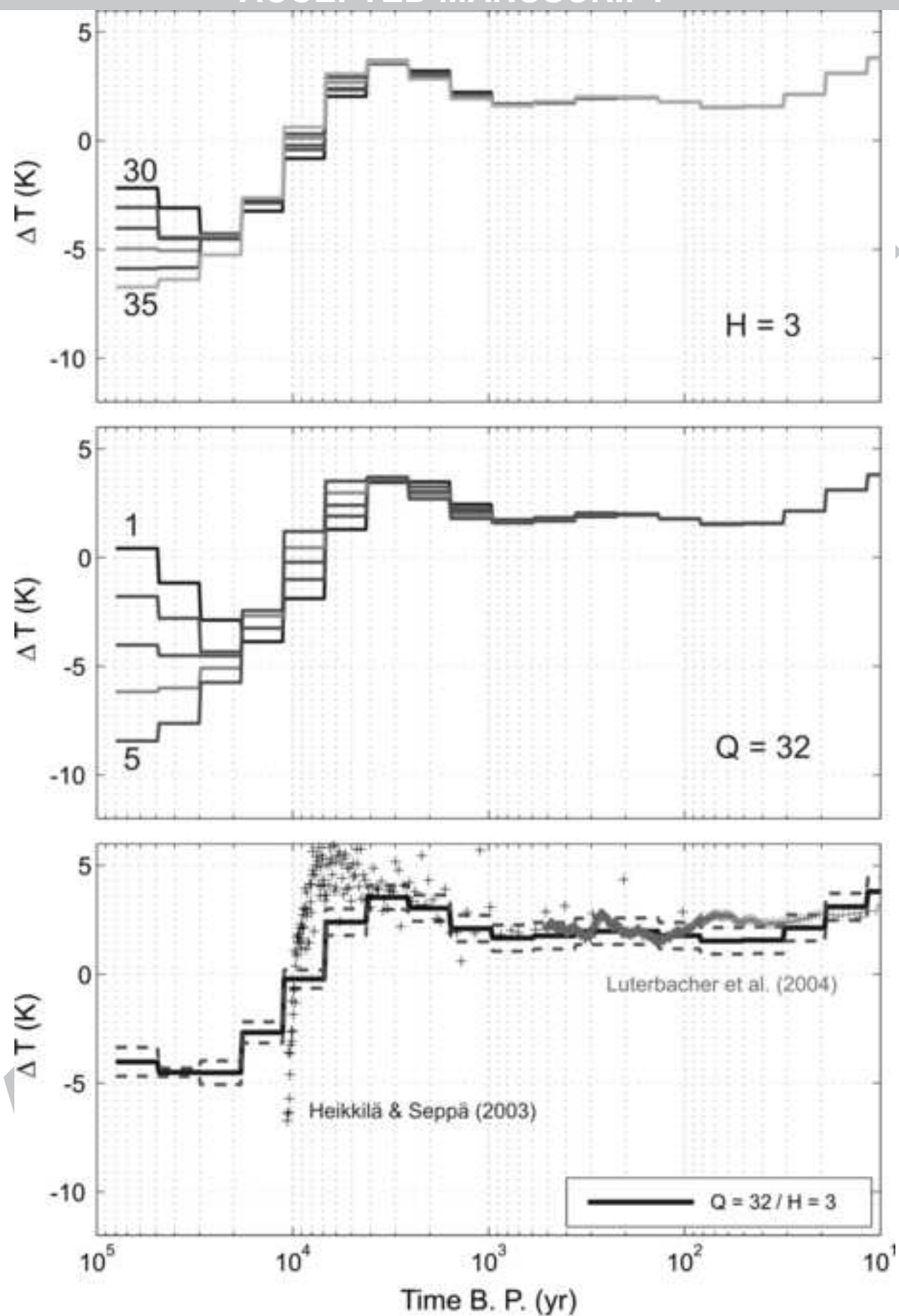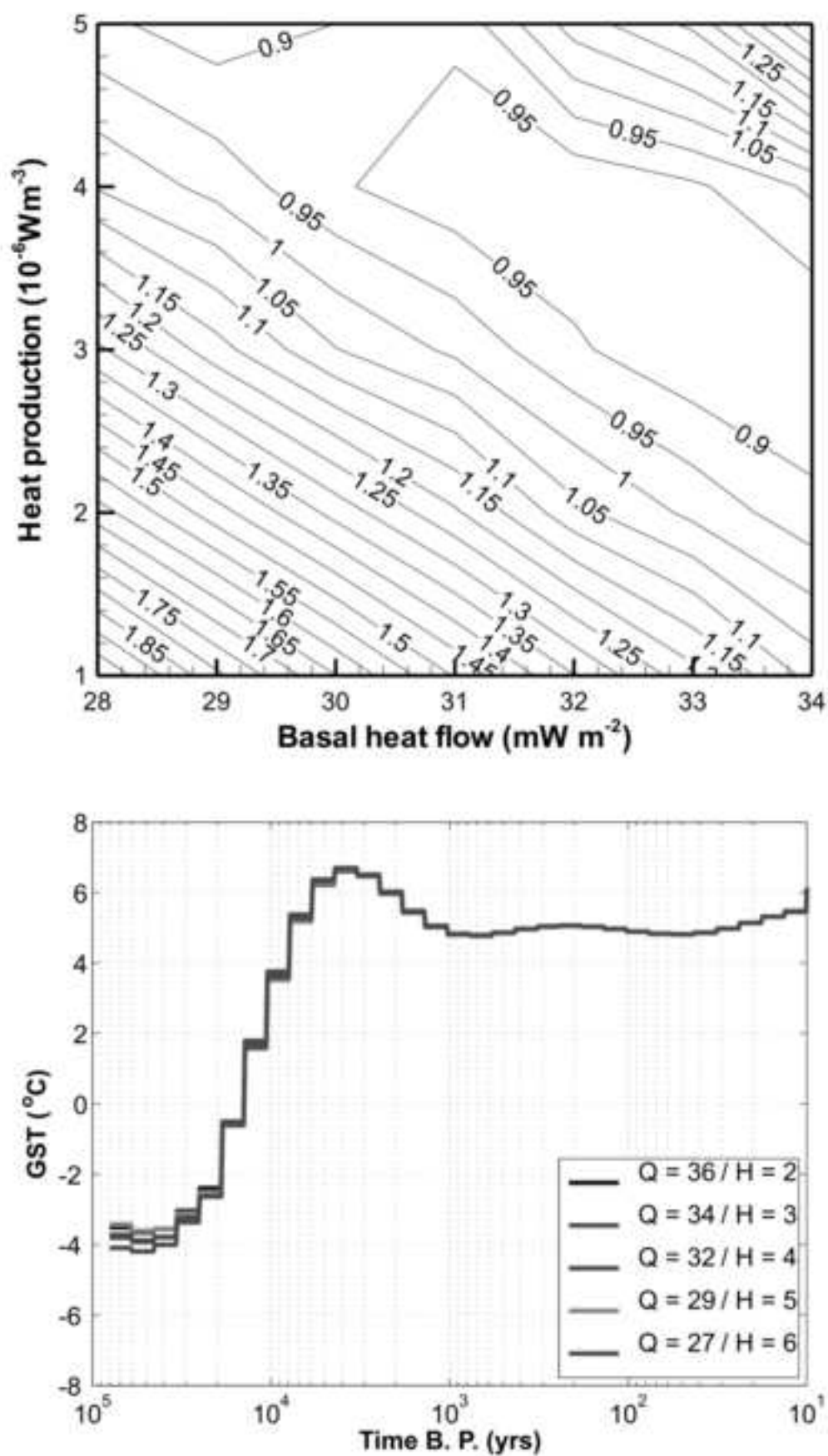
Fig. 10

Fig. 12

Fig. 13

Fig. 14
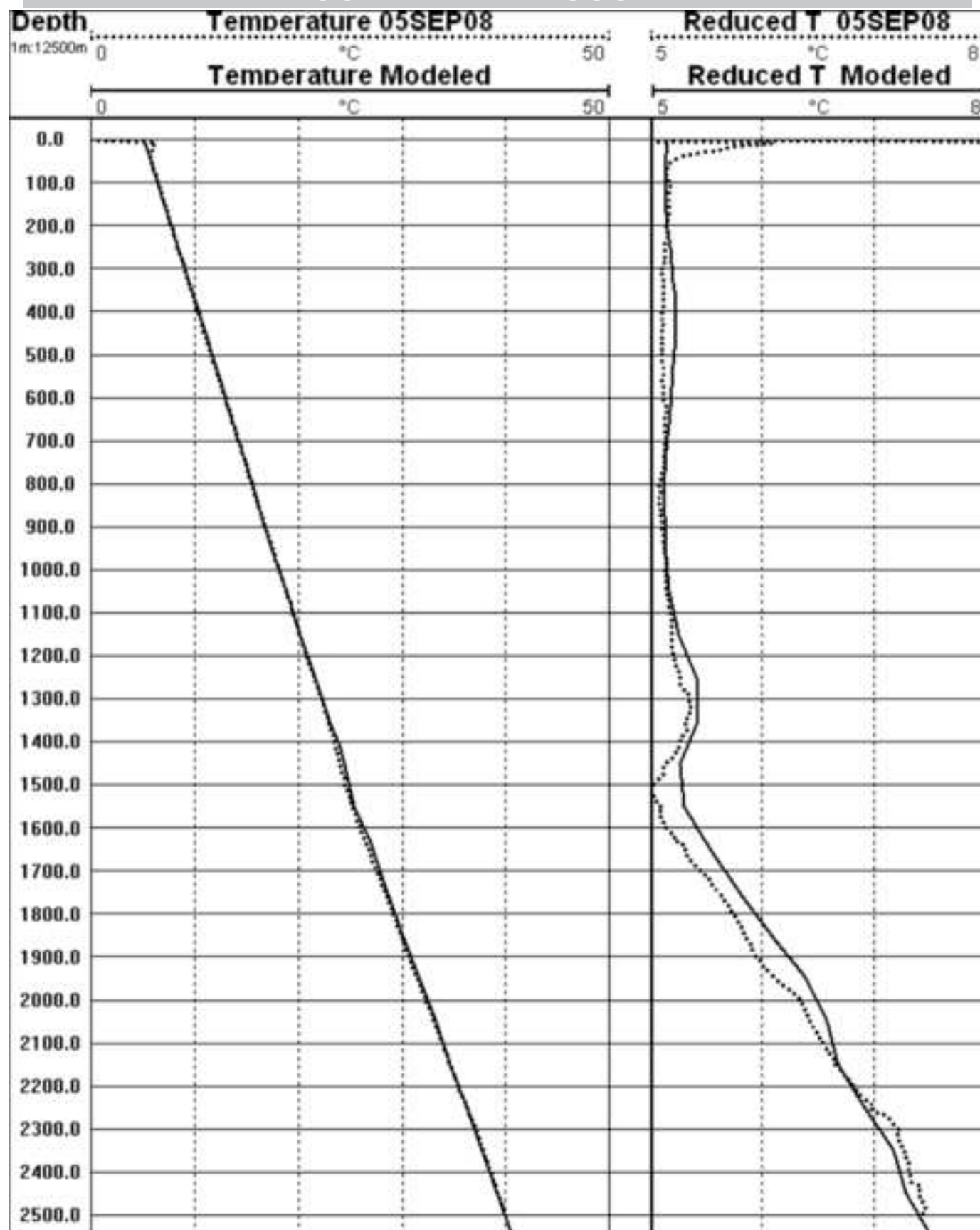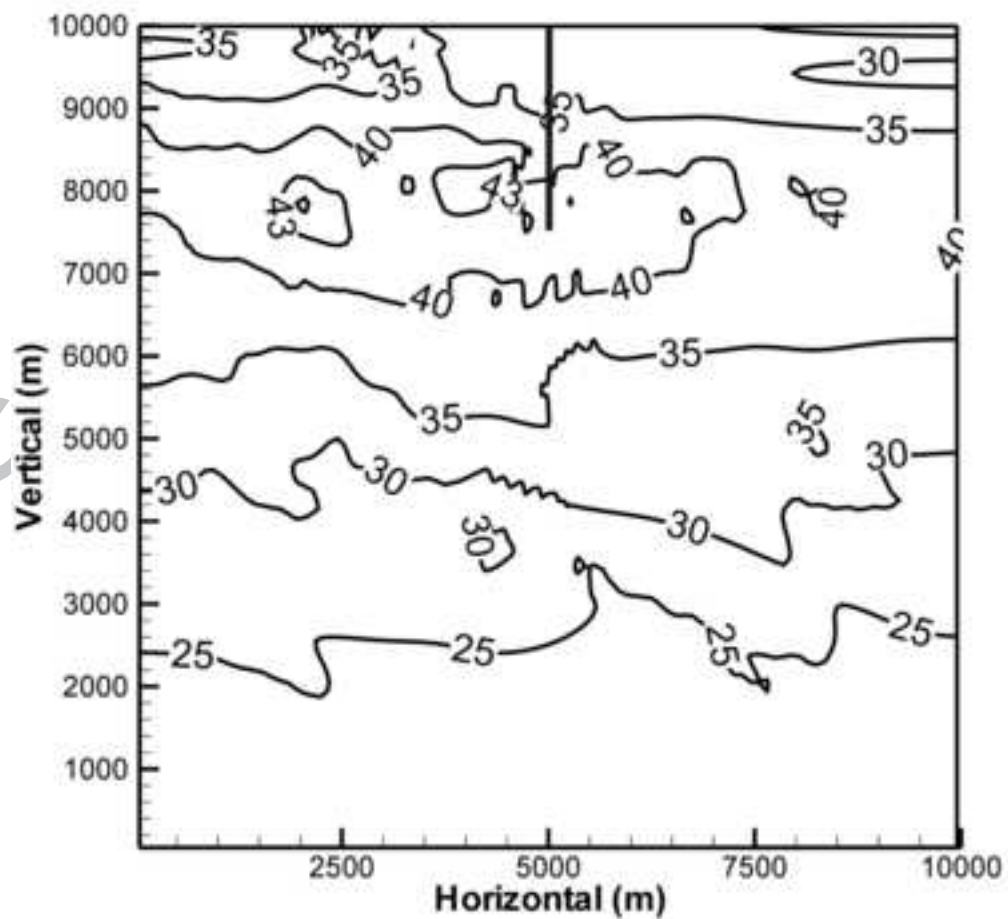
Table 1. Temperature logs of the Outokumpu deep drill hole.

Date	Activity	Drilling depth reached (m)	Shut-in time (days)	Max. logging depth (m)	Logger
Apr-6-2004	Start of drilling	0			
May-24-2004	Logging	550	1	550	NEDRA
Jul-15-2004	Logging	997	1	997	NEDRA
Sep-18-2004	Logging	1507	2	1507	NEDRA
Nov-11-2004	Logging	2073	1	2073	NEDRA
Jan-31-2005	End of drilling	2516			
Feb-7-2005	Logging	2516	7	2516	NEDRA
Aug-31-2005	Logging	2516	211	1418	GI-Prague
Apr-6-2006	Logging	2516	433	2508	ICDP-OSG
Sep-20-2006	Logging	2516	597	2507	ICDP-OSG
Sep-8-2008	Logging	2516	948	2503	ICDP-OSG

Table 2. Mean thermal conductivity, temperature gradient and heat flow density
of the Outokumpu deep drill hole calculated at 100 m intervals.

Depth interval	Conductivity	Standard dev.	Cond. mean error	N samples	T grad	Grad mean error
m	$Wm^{-1}K^{-1}$	$Wm^{-1}K^{-1}$	$Wm^{-1}K^{-1}$		$(mK\,m^{-1})$	$(mK\,m^{-1})$
50-100	2.28	1.13	0.36	10	12.58	0.04
100-200	2.47	0.65	0.11	37	12.77	0.00
200-300	2.47	0.40	0.06	51	12.63	0.01
300-400	2.44	0.50	0.06	75	13.08	0.01
400-500	2.35	0.46	0.05	76	12.92	0.01
500-600	2.48	0.52	0.06	88	13.22	0.01
600-700	2.48	0.40	0.06	51	13.04	0.01
700-800	2.50	0.58	0.06	96	12.53	0.01
800-900	2.44	0.74	0.08	91	13.14	0.01
900-1000	2.64	0.39	0.05	51	13.44	0.01
1000-1100	2.62	0.49	0.05	94	13.51	0.01
1100-1200	2.60	0.53	0.05	94	13.16	0.00
1200-1300	2.61	0.40	0.06	51	14.31	0.01
1300-1400	3.33	1.57	0.16	98	12.10	0.02
1400-1500	3.39	0.95	0.10	90	10.67	0.02
1500-1600	3.02	0.93	0.10	94	14.47	0.02
1600-1700	2.44	0.60	0.06	94	15.88	0.01
1700-1800	2.53	0.52	0.05	91	15.89	0.01
1800-1900	2.95	0.76	0.08	96	15.02	0.01
1900-2000	2.56	0.73	0.07	103	17.09	0.01
2000-2100	3.09	0.37	0.04	90	14.94	0.01
2100-2200	3.18	0.21	0.03	66	15.75	0.01
2200-2300	2.33	0.87	0.10	72	17.33	0.02
2300-2400	2.91	0.54	0.10	31	14.35	0.01
2400-2504	2.83	0.53	0.09	32	14.49	0.02

Table 3. Average values of thermal parameters in the Outokumpu deep hole.

Rock type	Conductivity $W\ m^{-1}K^{-1}$	Volumetric heat capacity $10^6\ J\ m^{-3}\ K^{-1}$	Heat production $\mu W\ m^{-3}$
Metasediments	2.50	1.89	1.70
Outokumpu assemblage[1]	3.35	2.11	1.55
Pegmatitic granite	3.00	1.78	5.40

[1]ophiolite-derived altered ultramafic rock types serpentinite, skarn rock, quartz rock

1280   Highlights
1281

- 1282   We study vertical variation in heat flow in Outokumpu, Fennoscandian shield,
  1283   in a 2.5 km deep hole.
- 1284   Heat flow increases from about 28-32 mW m^{-2} in the uppermost 1000 m to 40-
  1285   45 mW m^{-2} at depths >2000 m.
- 1286   It can be attributed to a palaeoclimatic effect due to ground surface
  1287   temperature (GST) variations during the last 100,000 years.
- 1288   The average GST was -3…-4°C during the Weichselian glaciation.
- 1289   Advective heat transfer was not observed and heat transfer is dominantly
  1290   conductive.

1291